REPORT DOCUMENTATION PAGE

Form Approved
OMB No. 0704-0188

1. AGENCY USE ONLY *(Leave blank)*	2. REPORT DATE	3. REPORT TYPE AND DATES COVERED
May 5, 1999	FINAL	15 Jan. 1996 – 31 March 1999

4. TITLE AND SUBTITLE

Degradation of haloaromatic compounds by indigenous sediment microflora: Biochemistry and molecular ecology.

5. FUNDING NUMBERS

N00014-96-1-0403

6. AUTHOR(S)

Lovell, Charles R.

7. PERFORMING ORGANIZATION NAME(S) AND ADDRESS(ES)

Department of Biological Sciences
University of South Carolina
Columbia, SC 29208

8. PERFORMING ORGANIZATION REPORT NUMBER

9. SPONSORING / MONITORING AGENCY NAME(S) AND ADDRESS(ES)

Office of Naval Research
800 N. Quincy St.
Arlington, VA 22217-5000

10. SPONSORING / MONITORING AGENCY REPORT NUMBER

11. SUPPLEMENTARY NOTES

12a. DISTRIBUTION / AVAILABILITY STATEMENT

Distribution unlimited

12b. DISTRIBUTION CODE

13. ABSTRACT ***(Maximum 200 words)***

This study examined microbial communities in biofilms lining marine infaunal burrows with particular focus on marine bacteria able to degrade chlorinated aromatic compounds. These biofilms contain a diverse and abundant microbiota, occurring as single cells and in microcolonial formations. The majority of these organisms are potentially active. The burrow biofilm microbiota includes bacteria able to remove halogen atoms from the aromatic ring of haloaromatic compounds. At least some of these bacteria are amenable to isolation and can be cultivated in the laboratory. Reductively dechlorinating bacteria were enriched from burrows produced by both haloaromatic producing and non-producing marine infauna. It is clear from these results that marine dechlorinating bacteria are common in infaunal burrow structures relative to bulk sediments. Two isolates able to debrominate bromophenols were characterized and identified as novel strains of *Propionigenium maris*. Microscopic examination also revealed the potential for interspecific interactions among dehalogenating bacteria and other types of organisms. These interactions may include consortial metabolism of chloroaromatics. The study revealed and characterized an important and previously unrecognized niche for reductively dehalogenating bacteria in marine sediments. Infaunal burrow structures provide a source for new organisms with potential application in bioremediation processes.

14. SUBJECT TERMS

Reductive dehalogenation, haloaromatics, infaunal burrows, biofilms, confocal scanning laser microscopy

15. NUMBER OF PAGES

16. PRICE CODE

17. SECURITY CLASSIFICATION OF REPORT	18. SECURITY CLASSIFICATION OF THIS PAGE	19. SECURITY CLASSIFICATION OF ABSTRACT	20. LIMITATION OF ABSTRACT
Unclassified	Unclassified	Unclassified	UL

FINAL REPORT

GRANT #: N00014-96-1-0403

PRINCIPAL INVESTIGATOR: Charles R. Lovell

INSTITUTION: University of South Carolina

GRANT TITLE: Degradation of haloaromatic compounds by indigenous marine sediment microflora: Biochemistry and molecular ecology.

AWARD PERIOD: 15 January 1996 - 31 March 1999

OBJECTIVES: To characterize microbial communities in biofilms lining marine infaunal burrows; to isolate new reductively dechlorinating marine bacteria from burrow lining biofilms; to determine microscale placement of reductive dechlorinators in biofilms.

APPROACH: Enrichment cultures providing a range of growth conditions were inoculated with burrow and tube lining biofilm material collected in the field from bromoaromatic producing *Balanoglossus aurantiacus*) and non-producing (*Kinbergonuphis jenneri*) infauna. These enrichments were screened for dechlorination of 2,4,6-trichlorophenol and were sources for isolation of dechlorinating pure cultures. The placement of microorganisms in tube lining biofilms has also been examined. Since various infaunal burrows and tubes support remarkably similar microbial communities, we have focused on a single model tube system constructed by the onuphid polychaete *Diopatra cuprea*. We used confocal scanning laser microscopy to visualize the microbiota in *Diopatra* tube biofilms and to determine which of these organisms are potentially active. A neural computing approach to analysis of phospholipid fatty acid profiles has been developed. Pure cultures of reductively debrominating marine bacteria have been characterized and the reductive debrominase they expressed examined.

ACCOMPLISHMENTS: Several enrichment culture series, prepared in 1997 and 1998 from field-collected samples of *K. jenneri* tubes and *B. aurantiacus* burrow linings, completely mineralized 2,4,6-trichlorophenol and yielded several anaerobic pure culture isolates that reductively dechlorinated this compound. These isolates lost the capacity to dechlorinate after several transfers. We tried a variety of vitamin supplements and basal medium recipes, but were unable to restore dechlorination activity to these isolates. New enrichments have been prepared using more restrictive medium recipes. These enrichments have performed well through initial transfers and have yielded one dechlorinating pure culture to date. This organism is currently being characterized and our isolation efforts are

continuing. We have completed the characterization of two reductively debrominating strains of *Propionigenium maris*. These cultures convert mM levels of 2,4,6-tribromophenol to 2- or 4-bromophenol and were isolated from the burrows of the hemichordate *B. aurantiacus* and the capitellid polychaete *Notomastus lobatus*. These strains differ in a number of structural and physiological characteristics from the *P. maris* type strain, particularly in the rapid debromination of 2,4,6-tribromophenol by our strains and the near absence of debromination by the type strain. Although these strains are distinguishable on the basis of several key characteristics, the 16S rRNA sequence homology among them is greater than 99%. This may indicate rapid evolution of burrow-associated *P. maris* strains. The reductive debrominase produced by these strains is cytoplasmic and can be reduced by both NADH and NADPH. There is no evidence for *P. maris* respiration using bromophenols as terminal electron acceptors.

We had previously examined the biofilms lining burrows and tubes of several polychaetes and hemichordates using phospholipid fatty acid (PLFA) analysis and have now employed a neural computing approach to resolve differences among PLFA profiles. This analytical method confirmed the similarity of bacterial communities in tubes and burrows of a variety of animals, allowing us to identify and focus on a single model infaunal tube system. We have chosen tubes constructed by a ubiquitous onuphid polychaete, *Diopatra cuprea*, as a model experimental system. This animal is found across a range of sediment types and can be collected from chronically contaminated sites. Tubes built by a related onuphid, *Kinbergonuphis jenneri*, have also been used in some experiments.

We have developed mounting and fluorescent staining methods for confocal scanning laser microscope examination of the biofilms lining *Diopatra cuprea* tubes. The average thickness of these biofilms was about 60 μm. No channels or channel-like structures, which are common in most laboratory-cultivated biofilms, were observed. Bacteria occurred as both single cells and microcolonies throughout the biofilm material. Single cell numbers averaged about $5.6 \times 10^8 \cdot cm^{-3}$ and the majority of these cells (ave. 68%) were intact, had membrane potential (as found using Syto 9/propidium iodide staining), and presumably capable of metabolic activity. No trends in active cell numbers with increasing depth in the biofilm were found, indicating potential for activity throughout the structure. Microcolony sizes were highly variable, ranging from 16 μm^3 to 2.5×10^5 μm^3. Single cell size (ave. = 0.085 μm^3) decreased and became more uniform with depth in the biofilm. *In situ* hybridization strategies for localization of reductively dechlorinating and other anaerobic bacteria have been developed.

CONCLUSIONS: Biofilms lining burrows and tubes constructed by marine infauna contain a diverse and abundant microbiota, occurring as single cells and in microcolonial formations. The majority of these organisms are at least potentially active. The burrow biofilm microbiota includes reductively dehalogenating bacteria, which can be readily enriched from burrow structures of several different infaunal species. At least some of these bacteria are amenable to isolation and can be cultivated in the laboratory. We have enriched reductively dechlorinating bacteria from burrows produced by both halometabolite producing and non-producing marine infauna. It is clear from these results that marine dechlorinating bacteria are common in infaunal burrow structures relative to bulk sediments. It is also clear from our microscopic examination of tube lining biofilms that the potential for interspecific interactions among dehalogenating bacteria and other types of organisms exists. These interactions may include consortial metabolism of chlorinated aromatic compounds by combinations of reductive dechlorinators and aromatic ring cleaving organisms.

SIGNIFICANCE: This study has revealed and characterized an important and previously unrecognized niche for reductively dehalogenating bacteria in marine sediments. Infaunal burrow structures provide a source for new organisms with potential application in bioremediation processes.

PATENT INFORMATION:

AWARD INFORMATION:

PUBLICATIONS AND ABSTRACTS:

1. Lovell, C.R., R.L. Marinelli, S.G. Wakeham, D.G. Ringelberg, and D.C. White (1998) Effects of host activities on the composition of microbial communities in biofilms lining burrows of marine infauna. Abstr. Gen. Meet. Am. Soc. Microbiol. N-135, p. 388.

2. Noble, P.A. and C.R. Lovell. Application of neural computing methods for interpreting phospholipid fatty acid profiles of natural microbial communities. Submitted to Appl. Environ. Microbiol.

3. Phillips, T.M. and C.R. Lovell (1998) Distribution of bacterial cells and biomass in *Diopatra cuprea* burrow lining biofilms. Abstr. Gen. Meet. Am. Soc. Microbiol. N-134, p. 388.

4. Phillips, T.M. and C.R. Lovell (1999) Distributions of total and active bacteria in biofilms lining tubes of the onuphid polychaete *Diopatra cuprea*. Mar. Ecol. Prog. Ser. In press.

5. Watson, J., G.Y. Matsui, J. Wiegel, F.A. Rainey, and C.R. Lovell. Reductively debrominating strains of *Propionigenium maris* from burrows of bromophenol producing marine infauna. Submitted to Internatl. J. Syst. Bacteriol.

Application of Neural Computing Methods For Interpreting Phospholipid Fatty Acid Profiles of Natural Microbial Communities

Peter A. Noble~* and Charles R. Lovell†*

LOVELL

~Corresponding Author

*Belle W. Baruch Institute for Marine Biology and Coastal Research,
University of South Carolina, Columbia, South Carolina 29208
Phone: 803-777-3928
FAX: 803-777-3935
Email: noble@biol.sc.edu

†Department of Biological Sciences
University of South Carolina,
Columbia, South Carolina 29208
Phone: 803-777-7036
FAX: 803-777-4002
Email:lovell@biol.sc.edu

Key words: PLFA, neural networks, hidden layer, microbial communities

Running title: Analysis of Microbial Community Compositions

ABSTRACT

The microbial community composition of surface and subsurface marine sediments, and sediments lining burrows of marine worms from the North Inlet estuary were analyzed by comparing ester-linked phospholipid fatty acid (PLFA) profiles using neural network (NN) and cluster analysis. PLFA profiles were converted to binary format for transmission to a back propagating NN. The NNs were trained to relate binary input to sample type (e.g., surface, subsurface, and burrow lining) and worm species (e.g., *Notomastus lobatus, Balanoglossus aurantiacus* and *Branchyoasychus americana*). The optimal architecture for the NN was found to be 540-input, 16-hidden and 4-output neurons. The optimal amount of training was found to be approximately 150 epochs (or to an error tolerance of 0.01). Results from cross-validation revealed that NNs were able to correctly discriminate microbial community profiles primarily by sample type (86.4%) rather than worm species (66.1%). Dendrograms produced by using Euclidean distance and average linkage clustering methods on data from five independently trained NNs yielded the following results. (i) PLFA profiles from microbial communities in the surface sediments were characterized by high levels of long-chain ($\geq$ 20 carbon units) polyunsaturated PLFAs and low levels of methyl-branched saturated PLFAs. (ii) Communities associated with subsurface sediments were characterized by low levels of polyunsaturated PLFAs and high levels of methyl-branched PLFAs. (iii) Sediments lining burrows of marine worms had PLFA profiles that were intermediate between these two extremes presumably reflecting the oxic/anoxic interface. The utility of NNs for interpreting complex PLFA profiles of microbial communities was demonstrated.

INTRODUCTION

Natural microbial communities are complex assemblages of organisms composed of a variety of different physiological groups of bacteria, archaea, and microeucaryotes, including fungi, algae and protozoa. Recent molecular biological studies have shown that the assemblage of organisms present in an environmental sample can contain thousands of distinct biotypes of bacteria (45, 46) and that many of these organisms represent undescribed microbial lineages, some of which lack even a single representative species available in pure culture (3). This complexity is further compounded by the high spatial and temporal variability of species represented in many natural communities (1, 6), and by the still open question of what proportion of the microscopically observable assemblage of organisms is viable or even metabolically functional (8, 29, 53). Characterization of natural microbial communities is clearly a difficult problem. Many molecular biological methods for community analysis are either very time consuming such as construction and screening of clonal libraries (3, 11, 20), or yield an index of community composition that does not reveal organism taxonomic affiliations without additional analysis, such as denaturing gradient gel electrophoresis (16, 34, 41). There is a clear need for methods than can be used to rapidly and accurately examine microbial community composition. Ideally, such methods would include all (or at least most) microbial domains and produce a standardizeable community profile, allowing comparisons across different sample types and facilitating development of broad hypotheses concerning microbial community dynamics.

One approach to microbial community characterization that has been successful in a wide variety of applications (e.g., 4, 5, 9, 18, 21, 35, 37, 43), is phospholipid fatty acid (PLFA) analysis (17). Phospholipids are structural components of all biological membranes. These compounds have no storage function and thus represent a consistent fraction of cell mass. They also degrade quickly upon an organism's death and current extraction and derivatization methods permit recovery of PLFAs exclusively from living organisms. Extraction and subsequent analysis by gas chromatography/mass spectroscopy provides precise resolution, sensitive detection, and accurate quantification of a broad array of PLFAs. Analyses can be performed rapidly and effficiently and each yields a profile composed of numerous PLFAs defined on the basis of compound structure and the quantity of each compound present in the sample. Different PLFA average chainlengths and degrees of unsaturation are produced by bacteria and eucarya, allowing both domains to be examined through the same analysis. The PLFA profile obtained thus

constitutes a 'fingerprint' of the living bacterial and microeucaryotic microbial community and reflects its species composition. Comparisons across sample types are simplified by normalizing the quantity of each PLFA to the total recovered, expressing the result in terms of mol% PLFA. One drawback of the PLFA analysis is that archaea are not represented in the analysis since their membrane lipids employ ether rather than ester bonds. Nonetheless, PLFA profiles can be used to characterize microbial community compositions and provide useful information on the dynamics of viable bacteria and microeucaryotes.

Comparing PLFA profiles of microbial communities is often complicated by variability in the types and quantities of compounds present in replicate samples from a given sample site. This, together with the complexity of the PLFA profiles, constitutes substantial challenges to our ability to quantitatively compare microbial community compositions using this approach. Previous studies have employed cluster analysis and principal components analysis (PCA) to group like samples (43) and to determine which PLFAs are most diagnostic for the groups defined (22, 25, 42). However, these methods do not permit details of the profiles to be conveniently examined. A method that provides the advantages of cluster analysis and PCA while facilitating more detailed profile examination would be very advantageous.

Artificial neural networks (NNs) provide an useful tool for recognizing patterns in complex data sets such as those associated with PLFA 'fingerprints'. NNs are constructed by using computer software and consist of layers of neurons that make independent computations and pass on their outputs to other neurons (36). Each neuron in a layer is connected to neurons in the next layer so that output of each neuron affects the activation of all neurons to which it is connected. Neurons are adaptable, and through the process of learning from examples, store knowledge and make it available for use (2). In a training technique called error back-propagation (38), a pattern is presented to an input layer of a network, and the network produces output based on the sum of the weighted inputs. When the pattern of the output layer is compared to target values, the errors between them are computed. An error function is used to readjust the weights of each neuron. This iterative process continues until the errors converge to a value below a designated tolerance level (38). The adjusted weights of a trained network can be used to recognize patterns such as those in PLFA profiles of microbial communities and to provide functional relations between profiles and target values.

There is a paucity of information concerning the effects of NN architecture and training on NN convergence and prediction. For the non-specialist, selecting the NN architecture and determining the amount of training needed for optimal performance of NNs has not been clearly established. For example, several studies have pointed out that having too many neurons in the hidden layer may cause unnecessary memorization of the training set (27, 28, 39, 51). As a consequence, the NN loses the capacity to generalize. Having too few neurons in the hidden layer results in non-convergence of the training set to the desired error tolerance. Overtraining NNs to low error tolerance values has similar consequences.

The focus of this study was to compare PLFA profiles of microbial communities in surface and subsurface nearshore sediments and in the linings of burrows of three species of marine worms by using a back-propagating neural network, and to outline the procedures needed to optimize NN performance. Optimization was achieved by varying the architecture and the extent of training and determining the effects of these factors on NN prediction. Here, we report on two different neural computing approaches for comparing PLFA profiles: cross-validation and cluster analysis using data from trained NN.

MATERIALS AND METHODS

Source of PLFA profiles analyzed. PLFA data used in our analyses were from a previous study of marine sediment microbiota by Steward et al. (42). This study should be consulted for sample site descriptions and significant features of the internal burrows sampled. Briefly, sediment samples collected for that study were ten matched sets for each of three worm species, with each set including: 1 worm burrow sediment sample, 1 surface sediment sample, and 1 subsurface sediment sample. Surface sediments were collected from approximately the top centimeter of sediment near but not adjacent to the worm burrows. Subsurface samples were taken approximately 10-20 cm deep, near but not adjacent to worm burrows. Sediments were scraped from the linings of burrows built by the capitellid polychaete *Notomastus lobatus* and the hemichordate *Balanoglossus aurantiacus* using sterile spatulas. Segments of tubes constructed by the maldanid polychaete *Branchyoasychus americana* were recovered intact. Large macrofauna were excluded from all samples. The samples were placed in sterile Whirlpack bags and immediately frozen on dry ice, then transferred to -80°C pending PLFA extraction and analysis as described by Steward et al. (42). This sample set included 90 total samples, each yielding a profile

of about 60 different fatty acids. Forty-two PLFAs were present at levels $\geq$ 0.01 mol% of most profiles accounted for 93-97% of total PLFA in each sample (42). The balance represented low abundance compounds.

Data for the NN. PLFA data used in this analysis also included control data which consisted of 23 randomly generated PLFA profiles. The limits of the random numbers were set by the maximum and minimum values of the PLFA data.

Input data for training the NN were generated by converting each of the 112 PLFA components to 9-digit binary numbers. This conversion set the maximum and minimium PLFA values to between '000000000' and '111111111', respectively. For example, if the quantity of the PLFA 16:0 was 2.71, the converted binary designation would be '000110000'. Input data for an entire microbial community in a sample consisted of 60 9-digit binary numbers ordered by their detection by the mass spectrophotometer.

Output data for training the NN related input data to sample type and sample group (by worm species) and was coded as a 4-digit binary number. The first 2-digits refer to the worm species and the next 2-digits refer to sample type. The worm species were coded '00', '10', '01' and '11' corresponding to the marine worms *B. aurantiacus, B. americana,* and *N. lobatus* and to randomly-generated data, respectively. The sample types were coded '01', '00', '10' and '11' and corresponding to surface, burrow, and subsurface samples, and randomly-generated data, respectively.

Input and output data used for training the NN consisted of the 60 9-digit binary numbers and the 4-digit binary output data. Data used for 'testing' the NN consisted of the 60 9-digit binary numbers only. To conform with the formating requirements of the NN program, spaces were inserted between each digit.

Cross-validation scheme. To evaluate the predictive power of the neural network, we employed the following cross-validation scheme: the order of the data were randomized, 75% of the data were used to train to an average error per sample of 0.01, and the remaining 25% were used to validate the NN performance. Correct and incorrect classifications were recorded. The above scheme was repeated 10 times for each cross-validation.

Optimization of the NN. The effects of architecture on the predictive accuracy of the NN were determined by independently training the NNs using 4, 8, 16, 64, or 270 neurons in the hidden layer. Unless otherwise specified, all NNs were trained to an error tolerance of 0.01 using a learning rate of 0.1, a momentum parameter of 0, and a noise factor of 0. Duplicate cross-validation experiments were used to evaluate the ability of trained NNs to relate PLFA profiles to

sample types and worm species.

To determine the effects of error tolerance level on the predictive accuracy of the NN, error tolerance values of 0.5, 0.1, 0.05, 0.01, 0.005, 0.001 and 0.0001 were used. For this experiment, the following NN architecture was used: 540-input, 16-hidden and 4-output neurons.

Phospholipid fatty acid nomenclature. Fatty acids are designated as A:BωC, where A is the total number of carbon atoms, B is the number of double bonds, and C is the position of the double bond from the aliphatic end of the molecule. Geometry of this bond is indicated 'c' for cis and 't' for trans. The prefixes 'i' and 'a' refer to iso and anteiso terminal methyl-branching respectively (26). Mid-chain methyl branches are designated by 'me' preceded by the position of the methyl group from the acid end of the molecule. Cyclopropyl fatty acids are designated as 'cy'.

Neural network software. The back-propagating neural network program used in this study has been previously described (see ref. 31). A binhex and binary version of this application is available through an anonymous ftp at inlet.geol.sc.edu. Additional software was needed to rapidly calculate the hidden layer data of trained NNs. The hidden layer data were used for cluster analysis. A stand-alone application for the Macintosh, called "hidden.app", was designed by using C++ software (Symantec, Release 5, Cupertino, CA). A binhex and binary version of this application is also available at our ftp site.

Numerical analysis. To evaluate the similarity of microbial communities from sample types and worm species, cluster analysis was performed, using the Euclidean distance coefficient and average linkage clustering methods (SPSS, Incorp.). The robustness of group memberships was determined by training the NN, calculating the hidden layer data, and performing cluster analyses. This process was repeated 5 times, resulting in the production of 5 dendrograms. Comparisons of cluster membership in the dendrogram enabled us to evaluate robustness of group memberships (15). To determine which of the PLFA molecules were common to the clusters, the mole percentage of PLFA data were imported into Transform 3.01 software (Spyglass, Inc., Savoy, IL).

RESULTS

Optimization of the neural network. The effects of architecture on the predictive abilities of NNs were determined by changing the number of hidden layer neurons in NNs and calculating the percent of correct predictions for both sample types and worm species (Table 1). It is important to

recognize that the NNs used in this experiment had the same number of input and output neurons but different numbers of hidden layer neurons. Each of the 10 trained NNs used to evaluate predictive power of NNs were trained on data different from those they were tested on. Moreover, each cross-validation procedure was performed in duplicate to provide a measure of the prediction variability. Increasing the number of hidden layer neurons in the NN decreased the number of epochs (i.e., number of completed training cycles) required to reach the desired error tolerance (Table 1). The results showed that the number of neurons in the hidden layer have a direct effect on the learning ability of NNs. NNs having too few hidden layer neurons (e.g., 4 hidden layer neurons) did not converge to the error tolerance of 0.01, indicating that the NN was not able to recognize patterns in the "fingerprints". Although increasing the number of neurons in the hidden layer decreased the mean number of epochs required to reach the desired error tolerance, the NN required more computation time to reach the desired error tolerance (data not shown).

Increasing the number of hidden layer neurons in the NNs did not necessarily improve the number of correct predictions. As indicated in Table 1, eight or more hidden layer neurons improved the number of correct predictions made by the NNs. However, having more than 64 hidden layer neurons did not significantly improve NN predictive power for either sample type or worm species. For sample type, the highest number of correct predictions occurred when the number of hidden layer neurons equalled 16 (Table 1). For worm species, the highest number of correct predictions occurred when 64 hidden layer neurons were used to train the NN (Table 1). For subsequent experiments, the following architecture was used: 540-input, 16-hidden, and 4-output neurons.

We investigated the effects of different error tolerance on the predictive abilities of NNs to establish the optimal number of epochs needed for training NNs. Decreasing the error tolerance values increased the number of epochs required to train the NNs (Fig. 1A) and therefore, the amount of computational time (data not shown). However, the percent of correct predictions did not significantly improve beyond an error tolerance of 0.01 (Fig. 1B). Presumably, beyond this threshold, the NNs lost their ability to generalize patterns in the PLFA profiles. Based on these data, the error tolerance of subsequent experiments was set at 0.01.

Cross-validation of the microbial communities. Examination of the NN predictions revealed that sample type (86.4 %) was more often correctly predicted than worm species (63.6%), indicating that microbial community compositions were more determined by whether or not they

were from the surface, burrow or subsurface than a particular worm species (Table 2). Incorrect predictions provide information on PLFA profiles having common characteristics. The overlap between microbial communities predicted for burrow and subsurface types, and burrow and surface types are presumably due to aberrant samples (see ref. 42) since there was little or no overlap between surface and subsurface samples. These results indicated that microbial communities among the sample types are distinctly different while those among the worm species are quite similar (Table 2).

Cluster analysis of the microbial community PLFA profiles. A dendrogram showing the relationship between microbial communities and their corresponding PLFA profiles is shown in Figure 2. The dendrogram represents the analysis of data from one hidden layer of one NN that was trained using 100% of the PLFA data. We compared the dendrogram (Fig. 2) to those obtained by analyzing the data from four additional independently trained NNs (data not shown). Although weights of the hidden layer changed every time the NNs were trained, these data yielded similar, but not identical dendrograms, indicating that group memberships for most samples were robust. Randomly-generated samples clustered separately from the rest of the clusters and formed a tight cluster at a rescaled similarity coefficient of ca. 87 in all dendrograms. This coefficient was used to group the profiles into clusters.

Based on the composition of the clusters in Figure 2, group memberships appeared to be determined by both sample type and worm species. However, the other dendrograms support the cross-validation results that sample type has a much greater effect on cluster membership than worm species. Comparison of the clusters to their corresponding PLFA profiles revealed which PLFA classes and which individual PLFAs were common to a given cluster (Fig. 2) and allowed some broad conclusions on PLFA distributions to be reached. Specifically, surface sediments characteristically contained high levels of long chain (i.e., greater than or equal to 20 carbon units in length) saturated and polyunsaturated fatty acids, indicative of microeucaryotes (14, 30, 33, 40, 48, 49, 50, 52), and low levels of terminally and mid-chain branched saturated and cyclopropyl fatty acids, indicative of low levels of anaerobic and/or gram positive bacteria (12, 13, 44, 47). Subsurface sediments showed the opposite trend, with generally low levels of long chain fatty acids and high levels of branched fatty acids. Burrow samples had PLFA profiles intermediate between these two extremes, reflecting the oxic/anoxic interface microenvironment burrows and tubes represent. Another indication of this is the relatively high abundance of cyclopropyl fatty

acids, particularly in *B. americana* tubes. Cylcopropyl fatty acids are often associated with oxic/anoxic interface environments (22).

DISCUSSION

In this study, two neural computing approaches were used to recognize patterns in the PLFA data of microbial communities: cross-validation of the NNs' predictions and cluster analysis of the hidden layer of trained NNs. To our knowledge, this is the first study to use two different neural computing approaches for examining complex PLFA patterns of natural microbial communities. We employed a statistical cross-validation scheme to provide information on the true predictive capabilities of NNs and cluster analysis of the hidden layer data of trained NNs to determine the relative similarities of PLFA profiles among the samples. This study and a previous study (31) have shown that cluster memberships of samples were robust and similar regardless of which hidden layer was used for cluster analysis, indicating that our approach was valid. The dendrograms were similar, but not identical, for different hidden-layer data because the weights change every time the NN was trained and the weights were randomized in the first training cycle. By comparing an image of the PLFA data to its corresponding dendrogram (Fig. 2), we determined which patterns in the microbial communities were common to the clusters, providing insight into the characteristics likely used by the NN to classify the PLFA data.

This study also used the cross-validation approach to optimize the architecture of the NN and to determine the extent of training required to most accurately predict the sample type and worm species. The NN architecture affected the mean number of epochs required to train the NN as well as the number of correct predictions. For a back-propagating NN, such as the one used in this study, variation in the NN architecture is primarily limited to changing the number of hidden layer neurons and/or the number of hidden layers since the number of input and output neurons are fixed by the number of digits in the raw data. We used one hidden layer because preliminary results (this study; 28) showed that more than one hidden layer was rarely beneficial. A low number of hidden layer neurons increased the number of epochs needed to train the NN and decreased the percent of correct predictions presumably because the NN did not have enough neurons to generalize the PLFA profiles. Similar results were obtained by Weinstein et al. (51). Having more than 64 hidden layer neurons also did not improve the percent of correct predictions (Table 1), indicating that the NN may have lost its ability to generalize. Choosing the appropriate

number of hidden layer neurons therefore, is extremely important for optimizing NN performance.

The application of neural computing approaches to analyze complex data is relatively new in microbiology. For example, NNs have been used to identify the restriction enzyme patterns of *Escherichia coli* 0157:H7 (10), the pyrolysis mass spectra of *Mycobacterium tuberculosis* complex species (19), the promoter sites of *E. coli* (23, 24), protein-DNA binding sites (32), fatty acids of marine heterotrophic bacteria (7), and stable low-molecular weight rRNA (31). The advantage of using neural computing approaches is that they allow pattern recognition that cannot be substantiated by standard statistical methods (28). This method also provides numeric and graphic information facilitating interpretation of PLFA data for the analysis of natural microbial communities.

ACKNOWLEDGMENTS

We thank Paula van Schie, M. Caroline Roper, Wes R. Johnson, and Maria E. Kitchens for proof reading the manuscript. This research was supported by the Office of Naval Research, grant number N000149610403 to C.R.L. This is contribution number XXXX of the Belle W. Baruch Institute for Marine Biology and Coastal Research.

REFERENCES

1. **Acinas, S.G., F. RodriguezValera, and C. PedrosAlio.** 1997. Spatial and temporal variation in marine bacterioplankton diversity as shown by RFLP fingerprinting of PCR amplified 16s rDNA. FEMS Microbiol. Ecol. **24**:27-40.

2. **Aleksander, I. and H. Morton.** 1991. Principles and promises. p.1-20. *In* I. Aleksander and H. Morton., An introduction to neural computing. Chapman & Hall, Ltd., London.

3. **Amann, R.I., W. Ludwig, and K.H. Schleifer.** 1995. Phylogenetic identification and *in-situ* detection of individual microbial-cells without cultivation. Microbiol. Rev. **59**: 143-169.

4. **Baird, B.H., and D.C. White.** 1985. Biomass and community structure of the abyssal microbiota determined from the ester-linked phospholipids recovered from Venezuela Basin and Puerto Rico Trench sediment. Mar. Geol. **68**:217-231.

5. **Balkwill, D.L, E.M. Murphy, D.M. Fair, D.B. Ringelberg, and D.C. White.** 1998. Microbial communities in high and low recharge environments: implications for microbial transport in the vadose zone. Microb. Ecol. **35**:156-171.

6. **Berardesco, G., S. Dyhrman, E. Gallagher, and M.P. Shiaris.** 1998. Spatial and temporal variation of phenanthrene-degrading bacteria in intertidal sediments. Appl. Environ. Microbiol. **64**:2560-2565.

7. **Bertone, S., M. Giacomini, C. Ruggiero, C. Piccarolo, and L. Calegari.** 1996. Automated systems for identification of heterotrophic marine bacteria on the basis of their fatty acid composition. Appl. Environ. Microbiol. **62**:2122-2132.

8. **Bogosian, G., P.J.L. Morris, and J.P. O'Neil.** 1998. A mixed culture recovery method indicates that enteric bacteria do not enter the viable but nonculturable state. Appl. Environ. Microbiol. **64**:1736-1742.

9. **Bossio, D.A., K.M. Scow, N. Gunapala, and K.J. Graham.** 1998. Determinants of soil microbial communities: Effects of agricultural management, season, and soil type on phospholipid fatty acid profiles. Microb. Ecol.**36**:1-12.

10. **Carson, C. A., J. M. Keller, K.K. McAdoo, D. Wang, B. Higgins, C.W. Bailey, J.G. Thorne, B.J. Payne, M. Skala and A.W. Hahn.** 1995. *Escherichia coli* O157:H7 restriction pattern recognition by artificial neural networks. J. Clin. Microbiol. **33**:2894-2898.

11. **Chandler, D.P., F.J. Brockman, and J.K. Fredrickson.** 1997. Use of 16s rDNA clone libraries to study changes in a microbial community resulting from *ex situ* perturbation of a subsurface sediment. FEMS Microbiol. Rev. **20**:217-230.

12. **Dowling, N.J.E., F. Widdel, and D.C. White.** 1986. Phospholipid ester-linked fatty acid biomarkers of acetate-oxidizing sulphate-reducers and other sulphide-forming bacteria. J. Gen. Microbiol. **132**:1815-1825.

13. **Edlund, A., P.D. Nichols, R. Roffey, and D.C. White.** 1985. Extractable and lipopolysaccharide fatty acid hydroxy acid profiles from *Desulfovibrio* species. J. Lipid. Res. **26**:982-988.

14. **Erwin, J.A.** 1973. Comparative biochemstry of fatty acids in eukaryotic microorganisms, p. 41-43. In J.A. Erwin (ed.) Lipids and biomembrances of eukayotic microorganisms. Academic Press, New York.

15. **Everitt, B.S.** 1974. Cluster analysis. Wiley and Sons, New York, N.Y.

16. **Ferris, M.J., and D.M. Ward.** 1997. Seasonal distributions of dominant 16S rRNA-defined populations in a hot spring microbial mat examined by denaturing gradient gel electrophoresis. Appl. Environ. Microbiol. **63**:1375-1381.

17. **Findlay, R.H., and F.C. Dobbs.** 1993. Quantitative description of microbial communities using lipid analysis, p. 271-284. In P.R. Kemp, B.F. Sherr, E.B. Sherr, and J.J. Cole (ed.), Handbook of methods in aquatic microbial ecology. Lewis, Boca Raton, Fla.

18. **Findlay, R.H., B. Trexler, J.B. Guckert, and D.C. White.** 1990. Laboratory study of disturbance in marine sediments: response of a microbial community. Mar. Ecol. Prog. Ser. **62**:121-133.

19. **Freeman, R., R. Goodacre, P.R. Sisson, J.G. Magee, A.C. Ward, and N.F. Lightfoot.** 1994. Rapid identification of species within the *Mycobacterium tuberculosis* complex by artificial neural network analysis of pyrolysis mass spectra. J. Med. Microbiol. **40**:170-173.

20. **Gray, J.P. and R.P. Herwig.** 1996. Phylogenetic analysis of the bacterial communities in marine sediments. Appl. Environ. Microbiol. **62**:4049-4059.

21. **Guckert, J.B., C.P. Antworth, P.D. Nichols, and D.C. White.** 1985. Phospholipid, ester-linked fatty acid profiles as reproducible assays for changes in prokaryotic community structure of estuarine sediments. FEMS Microbiol. Ecol. **31**:147-158.

22. **Guckert, J.B., D.B. Ringelberg, D.C. White, R.S. Hanson, and B.J. Bratina.** 1991. Membrane fatty-acids as phenotypic markers in the polyphasic taxonomy of methylotrophs within the proteobacteria. J. Gen. Microbiol. **137**:2631-2641.

23. **Hertz, G.Z., and G.D. Stormo.** 1996. *Escherichia coli* promoter sequences: Analysis and prediction. Method Enzymol . **273**:30-42.

24. **Horton, P.B. and M. Kanehisa.** 1992. An assessment of neural networks and statistical approaches for prediction of *E. coli* promoter sites. Nucleic Acids Res. **20**:4331-4338.

25. **Ibekwe, A.M., and A.C. Kennedy.** 1998. Phospholipid fatty acid profiles and carbon utilization patterns for analysis of microbial community structure under field and greenhouse conditions. FEMS Microbiol. Ecol. **26**:151-163.

26. **Kates, M.** 1986. Techniques in lipidology: Isolation, analysis and identification of lipids. 2nd ed. Elsevier, Amsterdam.

27. **Maier, H.R., G.C. Dandy, and M.D. Burch.** 1998. Use of artificial neural networks for modelling cyanobacteria Anabaena spp. in the River Murray, South Australia. Ecol. Model. **105**:257-272

28. **Masters, T.** 1993. Practical neural network recipes in C++. Academic Press, New York, N.Y.

29. **McDougald, D., S.A. Rice, D. Weichart, and S. Kjelleberg.** 1998. Nonculturability: adaptation or debilitation? FEMS Microbiol. Ecol. **25**:1-9.

30. **Nichols, P.D., A.C. Palmisino, G.A. Smith, and D.C. White.** 1986. Lipids of the antarctic sea ice diatom *Nitzschia cylindrus*. Phytochemistry **25**:1649-1653.

31. **Noble, P.A., K.D. Bidle and M. Fletcher.** 1997. Natural microbial community compositions compared by a back-propagating neural network and cluster analysis of 5S rRNA. Appl. Environ. Microbiol. **63**:1762-1770.

32. **O'Neill, M.C.** 1998. A general procedure for locating and analyzing protein-binding sequence motifs in nucleic acids. Proc. Natl. Acad. Sci. **95**:10710-10715.

33. **Orcutt, D.M. amd G.W. Patterson.** 1975. Sterol, fatty acid and elemental composition of diatoms grown in chemically defined media. Comp. Biochem. Physiol. **50B**:579-583.

34. **Ovreas, L., L. Forney, F.L. Daae, and V. Torsvik.** 1997. Distribution of bacterioplankton in meromictic lake Saelenvannet, as determined by denaturing gradient gel electrophoresis of PCR-amplified gene fragments coding for 16s rRNA. Appl. Environ. Microbiol. **63**:3367-3373.

35. **Rajendran, N., O. Matsuda, N. Imamura, and Y. Urushigawa.** 1992. Variation in microbial biomass and community structure in sediments of eutrophic bays as determined by phospholipid ester-linked fatty acids. Appl. Environ. Microbiol. **58**:562-571.

36. **Rao, V. B. and H.V. Rao.** 1993. C++ Neural networks and fuzzy logic. MIS:Press, New York, NY.

37. **Ringelberg, D.B.,S. Sutton, and D.C. White.** 1997. Biomass, bioactivity and biodiversity: microbial ecology of the deep subsurface: analysis of ester-linked phospholipid fatty acids. FEMS Microbiol. Rev. **20**:371-377.

38. **Rumelhart, D. E, G. E. Hinton and R. J. Williams.** 1986. Learning internal representation by error back propagation, p. 318-362. *In* D. E. Rumelhart and J. L. McCleland (ed.), Parallel distributed processing. M.I.T. Press, Cambridge, Mass.

39. **Simpson, R., R. Williams, R. Ellis and R.F. Culverhouse.** 1992. Biological pattern recognition by neural networks. Mar. Ecol. Prog. Ser. **79**:303-308.

40. **Smith, G.A., P.D. Nichols, and D.C. White.** 1986. Fatty acid composition and microbial activity of benthic marine sediment from McMurdo Sound, Antarctica. FEMS Microbiol. Ecol. **38**:219-231.

41. **Stephen, J.R., G.A. Kowalchuk, M.A.V. Bruns, A.E. McCaig, C.J. Phillips, T.M. Embley, and J.I. Prosser.** 1998. Analysis of beta-subgroup proteobacterial ammonia oxidizer populations in soil by denaturing gradient gel electrophoresis analysis and hierarchical phylogenetic probing. Appl. Environ. Microbiol. **64**:2958-2965.

42. **Steward, C.C., S.C. Nold, D.B. Ringelberg, D.C. White, and C.R. Lovell.** 1996. Microbial biomass and community structures in the burrows of bromophenol producing and non-producing marine worms and surrounding sediments. Mar. Ecol. Prog. Ser. **133**:149-165.

43. **Sundh, I., M. Nilsson, and P. Borga.** 1997. Variation in microbial community structure in two boreal peatlands as determined by analysis of phospholipid fatty acid profiles. Appl. Environ. Microbiol. **63**:1476-1482.

44. **Taylor, J. and R.J. Parkes.** 1983. The cellular fatty acids of the sulphate-reducing bacteria, *Desulfobacter* sp., *Desulfobulbus* sp., and *Desulfovibrio desulfuricans.* J. Gen. Microbiol. **129**:3303-3309.

45. **Torsvik, V., J. Goksoyr, and F.L. Daae.** 1990. High diversity in DNA of soil bacteria. Appl. Environ. Microbiol. **56**:782-787.

46. **Torsvik, V., K. Salte, R. Sorheim, and J. Goksoyr.** 1990. Comparison of phenotypic diversity and DNA heterogeneity in a population of soil bacteria. Appl. Environ. Microbiol. **56**:776-781.

47. **Vainshtein, M., H. Hippe, and R.M. Kroppenstedt.** 1992. Cellular fatty acid composition of *Desulfovibrio* species and its use in classification of sulfate-reducing bacteria. Syst. Appl. Microbiol. **15**:554-566.

48. **Vestal, R.J. and D.C. White.** 1989. Lipid analysis in microbial ecology: quantitative approaches to the study of microbial communities. BioSci. **39**:535-541.

49. **Volkman, J.K. and R.B. Johns.** 1977. The geochemical significance of positional isomers of unsaturated acids from an intertidal zone sediment. Nature. **267**:693-694.

50. **Volkman, J.K., R.B. Johns, F.T. Gillan, G.J. Perry, and H.J. Bavor.** 1980. Microbial lipids of an intertidal sediment. I. Fatty acids and hydrocarbons. Geochim. Cosmochim. Acta. **44**:1133-1143.

51. **Weinstein, J.N., K.W. Kohn, M.R. Grever, V.N. Viswanadhan, L.V. Rubinstein, A.P. Monks, D.A. Scudiero, L. Welch, A.D. Koutsoukps, A. J. Chiausa, and K.D. Paull.** 1992. Neural computing in cancer drug development: predicting mechanism of action. Science. **258**:447-451.

52. **White, D.C.** 1983. Analysis of microorganisms in terms of quantity and activity in natural environments. p. 37-66. *In* J.H. Slater, R. Whittenbury, and J.W.T. Wimpenny (eds.) Microbes in their natural environments. Symp. Soc. Gen. Microbiol. 34. Cambridge University Press, Cambridge.

53. **Zweifel, U. L., and Å. Hagström.** 1995. Total counts of marine bacteria include a large fraction of non-nucleoid-containing bacteria (ghosts). Appl. Environ. Microbiol. **64**:2180-2185.

FIGURE LEGENDS

Figure 1. Relationship of error tolerance to epochs (A) and to percent correct predictions (B). Each circle represents the result of one cross-validation experiment. Open and closed circles in B represent correct predictions for sample type and worm species, respectively.

Figure 2. A dendrogram showing the relationships of microbial communities from collected samples and their corresponding PLFA profiles. The similarity scores of the 112 samples were determined by calculating the squared Euclidean distance and clustering the data using average distance linkage methods. The 23 randomly-generated samples are represented by the letter R. Black, gray and white symbols represent burrow, surface and subsurface sample types, respectively. Circles, squares and triangles represent *Branchiasychus americana, Balanoglossus aurantiacus,* and *Notomastus lobatus,* respectively. Each PLFA molecule is represented by a box in the "fingerprint" image, whose shade is based on phospholipid fatty acid mol% values; white and dark boxes representing low (0) and high intensities ($\geq$5), respectively. The order of the PLFA are as follows: saturated, 14:0, 15:0, 16:0, 17:0, 18:0, 20:0, 22:0, 24:0; branched saturated, i14:0, i15:0, a15:0, i16:0, i17:0, 17:1ω8c/a17:0; mono unsaturated a16:0/16:1ω9c, 16:1ω7c, 16:1ω7t, 16:1ω5c, 16:1ω13t, 17:1ω6c, 18:1ω7t, 16:2ω6/br15:0, 18:1ω9c, 18:1ω7c, 19:1ω12c, 19:1ω8c, 19:1ω6c, 20:1ω9c, 20:1ω7c; polyunsaturated, Poly 17 (2+ω), 18:3ω6/10Me17:0, 18:4ω3/12Me17:0, 18:2ω6, 18:3ω3/Br17:1/i18:0, 20:4ω6, 20:5ω3, 20:3ω6, 20:4ω3, 20:3ω3, 22:5ω6, 22:6ω3, 20:2ω6,22:4ω6, 22:5ω3, poly 19 (3+ω), Poly 22 (2ω); methyl-branched saturated, 10Me16:0, 10Me18:0, 11Me18:0; cyclopropyl, cy17:0, cy19:0 (ω7,8).

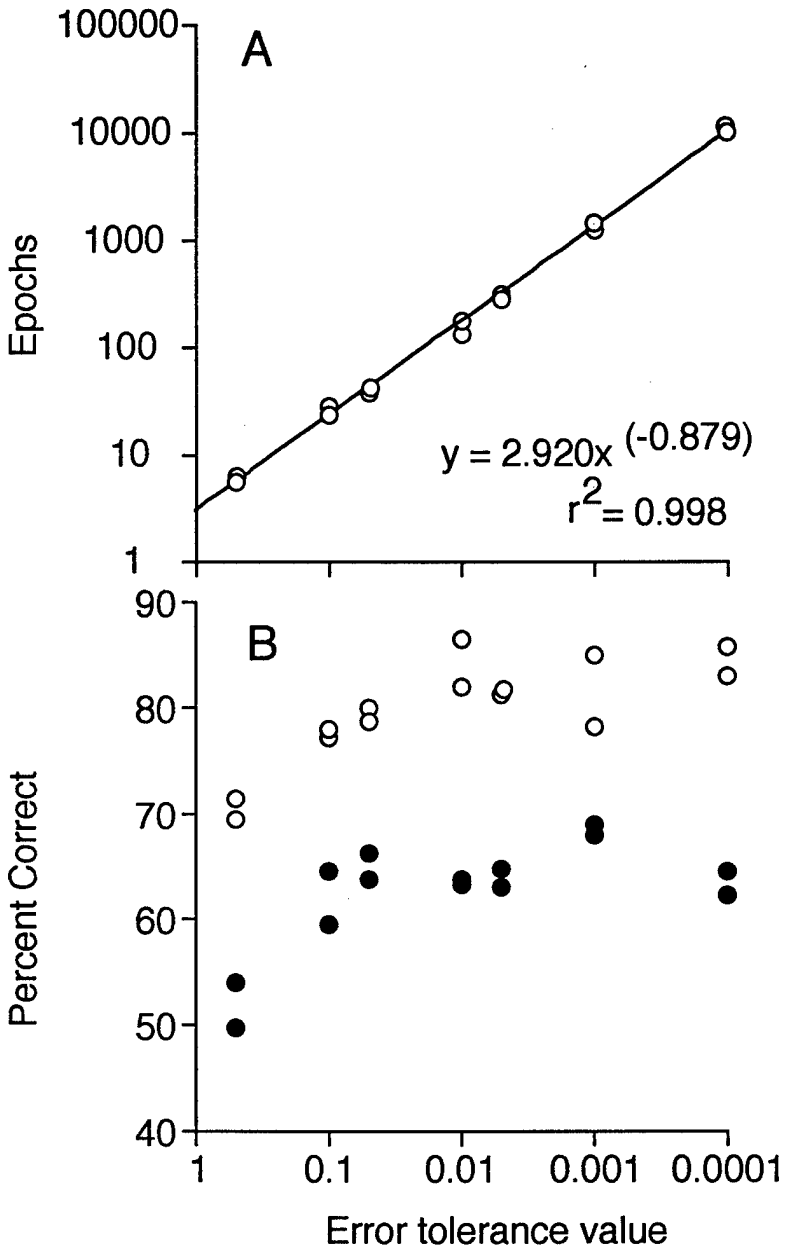
A
100000
10000
1000
100
10
1
Epochs
y = 2.920x (-0.879)
r2= 0.998
B
90
80
70
60
50
40
Percent Correct
1
0.1
0.01
0.001
0.0001
Error tolerance value

FIG 1.

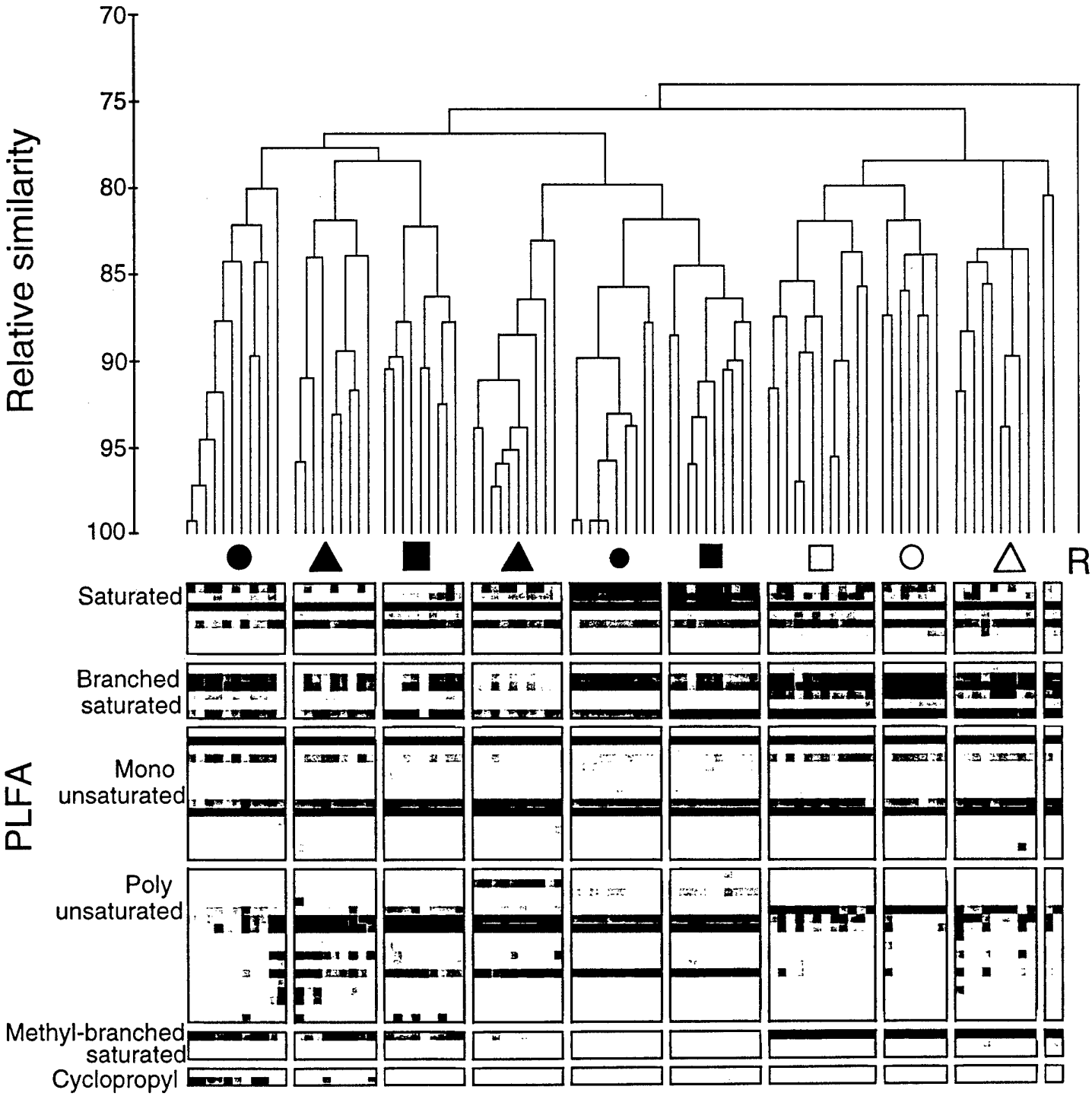
Relative similarity
70
75
80
85
90
95
100
R
PLFA
Saturated
Branched saturated
Mono unsaturated
Poly unsaturated
Methyl-branched saturated
Cyclopropyl

FIG 2

TABLE 1. Percentage of correct predictions of sample affiliations using back-propagating NNs with n -number of neurons in the hidden layer. The architecture of NNs were 540-input, n -hidden, and 4-output neurons and trained to an error tolerance value of 0.01.

n -number of neurons in the hidden layer	Mean epoch ± SD (n =2)	Percentage of correct sample type predictions by replicate:		Percentage of correct worm species predictions by replicate:	
		1	2	1	2
4	-[a]	-	-	-	-
8	368.4 ± 14.5	79.3[b]	82.9	62.9	62.1
16	149.7 ± 31.7	86.4	81.8	63.6	63.2
64	42.9 ± 1.2	84.3	84.6	65.4	66.1
270	8.3 ± 0.0	82.9	82.9	65.4	64.3

[a], NNs did not converge to an error tolerance value of 0.01.

[b], each datum is based on one cross-validation as outlined in Materials and Methods

TABLE 2. Prediction of microbial communities using back-propagating NNs with the architecture of 540-input, 16-hidden, and 4-output neurons and an error tolerance of 0.01. The left column gives the actual samples; numbers in bold are correct predictions; numbers not in bold are incorrect predictions. The total correct predictions for sample type was 242 (86.4%); the total of incorrect predictions was 38 (13.6%). The total correct predictions for worm species was 178 (63.6%); the total of incorrect predictions was 102 (36.4%).

Actual	Predicted samples by sample type and worm species:								
sample*	Burrow	Subsurface	Surface	Random	*B. aurantiacus*	*B. americana*	*N. lobatus*	Random	Total samples
Burrow	**60**	11	8						79
Subsurface	10	**54**	1						65
Surface	4		**67**	1					72
Random		1	2	**61**					64
B. aurantiacus					**40**	15	7	1	63
B. americana					30	**36**	9	2	77
N. lobatus					28	6	**41**	1	76
Random							3	**61**	64

*, Labels are designated in the text.

DISTRIBUTIONS OF TOTAL AND ACTIVE BACTERIA IN BIOFILMS LINING TUBES OF THE ONUPHID POLYCHAETE *DIOPATRA CUPREA*.

Tina M. Phillips and Charles R. Lovell[1]

Department of Biological Sciences

University of South Carolina

Columbia, SC 29208

USA

[1]Corresponding author phone: (803)777-7036

FAX: (803)777-4002

Email: lovell@biol.sc.edu

Running head: Bacterial distributions in *D. cuprea* tubes

Keywords: Microbial communities - infaunal burrows - spatial distributions – confocal scanning laser microscopy

ABSTRACT

Infaunal burrows and tubes support elevated levels of microbial biomass and activities relative to the surrounding bulk sediments. The impacts of these structures on sediment biogeochemistry have been intensively studied, but very little is known about the microbiota or their spatial organization within these microenvironments. Distributions of bacterial cells and microcolonies and of potentially active bacterial cells in tubes of the onuphid polychaete *Diopatra cuprea* were determined using confocal scanning laser microscopy. Distributions were examined among different tubes, at different locations within a tube, and at different depths in the biofilms lining these tubes. The average quantity of cells across all tubes examined was 5 .61 x 10^8 per cm^3 and there was no trend in the distribution of cells along the length of the tube or with increasing depth in the biofilm. Cell size across all tubes collected in February 1997 averaged 0.085 μm^3 but varied seasonally. Mean cell size increased with increasing depth below the sediment surface of the tube site sampled, and decreased with increasing depth in the biofilm. Microcolonies were abundant and not confined to specific depths within the biofilm or locations within the tube. Potentially active cells were observed at all depths within the biofilm and at least 46% (mean = 68%) of cells at any given site were potentially active. We hypothesize that the observed trends in cell distribution are responsive to tube irrigation by the host animal.

INTRODUCTION

Geochemical cycling of the major biogenic elements in nearshore marine sediments is primarily mediated by microorganisms. However, sediments are far from homogeneous and some specific microenvironments are particularly conducive to microbial activities. Chemocline environments, such as those found at the sediment-water interface, are well known to be sites of enhanced microbial activities (Novitsky 1983, Novitsky and Karl 1986). The classic model of these interface environments places aerobic metabolism at the sediment surface, followed by various anaerobic processes in deeper sediment layers (e.g. Aller 1988, Fenchel 1969, Revsbech and Jorgensen 1986). However, surface sediments are subject to high levels of disturbance due to physical and biogenic reworking (Grant 1983, Yingst and Rhoads 1980). Sediment mixing can greatly stimulate some microbial activities by increasing the quantities of potential electron donors and acceptors below the sediment-water interface (Findlay and White 1983, 1984, Findlay et al. 1990, Krantzberg 1985). Mixing also disrupts chemocline microbial communities and may significantly alter the interactions among various microbial functional groups and affect their potential for consortial metabolism (Paerl and Pinckney 1996).

Macrofaunal burrows and tubes also provide significant chemocline niches for microbial growth. These structures are dug into anoxic subsurface sediments, irrigated with oxic seawater, and provide a large surface area for diffusive exchange (Aller 1980, Aller and Yingst 1978, Boudreau and Marinelli 1994). Irrigation of the burrow by the

macrofaunal host organism results in the formation of radial chemoclines extending out from the burrow wall into the surrounding sediments (Aller 1983, 1988, Aller and Yingst 1978, Boudreau and Marinelli 1994, Marinelli and Boudreau 1996). These radial chemoclines provide overlapping gradients of potential electron donors and acceptors and are stable over time spans long enough for development of complex microbial communities (Aller and Aller 1986, Marinelli, Wakeham, Ringelberg, White, and Lovell, unpublished). Macrofaunal burrows vary in their structural properties, ranging from loosely packed sediment/mucopolysaccharide aggregates, as seen in the burrows of the terebellid polychaete *Amphitrite ornata*, to well-defined polysaccharide and/or proteinaceous tubes, such as those of the chaetopterid polychaete *Chaetopterus variopedatus* and the onuphid polychaete *Diopatra cuprea* (Aller 1983, Aller and Yingst 1978, Myers 1972). These structures promote development of microbial biofilms (Steward et al. 1996) containing high levels of microbial biomass and supporting intense geochemical cycling activities (Binnerup et al. 1992, Kristensen et al. 1985, 1991). Previous studies have shown that the microbiota of burrow lining biofilms differs from that of adjacent bulk sediments (Dobbs and Guckert 1988, Steward et al. 1996) and that burrow and tube microbiota play important roles in the mineralization of organic compounds and the geochemical cycling of biogenic elements (e.g. Binnerup et al. 1992, Kristensen et al. 1985, 1991). The rates of geochemical processes within the burrow biofilm rely mainly on the constituents of the microbial community and their levels of activity. The latter are obviously highly dependent on the properties of the burrow (stability and permeability) and on the irrigation and exudation activities of the host animal. However, the distributions and potential for consortial interactions of these

organisms are almost completely unknown and can best be studied using microscopic analysis.

Recent developments in microscopy, specifically confocal scanning laser microscopy, allow examination of bacterial biofilms in a non-invasive manner (Costerton et al. 1995). Studies to date have primarily examined biofilms grown on impermeable surfaces and little is known about natural biofilms growing on permeable surfaces and the microbiota inhabiting them. In this study we examined distributions of total and active bacterial cells in biofilms lining the stable tube structure constructed by a ubiquitous infaunal polychaete, *Diopatra cuprea*. Several key features of the tube lining biofilm microbiota were revealed.

CHARACTERISTICS OF THE *DIOPATRA CUPREA* TUBE

The *D. cuprea* tube is constructed from a mucous, sulphated polysaccharide, released from secreting glands, which hardens when it comes in contact with seawater (Myers 1972). Each tube displays two types of construction, reinforced and unreinforced (Figure 1). The reinforced section rises from the sediment surface and can also extend down into shallow subsurface sediments. The length of this section is dependent on the degree of sediment disturbance and the animal will extend it if the exposed portion becomes buried. The reinforced section of the tube is decorated with debris (small pebbles, shell fragments, and plant detritus) from the sediment surface. Occasionally,

tubes will have two reinforced openings. The unreinforced section occurs below the sediment surface and is constructed as the worm moves vertically down through the sediments, creating a mucous sheath. The only foreign materials that may be attached to this portion of the tube are sediment particles in direct contact with the mucus when it is secreted. Additional layers of mucus are laid within the tube over time, so the thickness of the tube is directly proportional to its age.

MATERIALS AND METHODS

Sampling site. *Diopatra cuprea* tubes were collected from an intertidal sandflat located at Oyster Landing, in the North Inlet saltmarsh (79°W, 33°N), near Georgetown, South Carolina, USA. Oyster Landing is a small tidal tributary bordered by *Spartina alterniflora* marsh and oyster beds (Allen et al. 1992, Lovell and Piceno 1994). The sandflat from which samples were collected is completely exposed during low tide and consists of quartz sand (median grain size of 376 μm) containing 0.22% silt and clay, and 0.83% organic matter, by dry weight (Lovell and Piceno 1994).

Sample collection. All *D. cuprea* tubes collected for this study were built by solitary individuals and had no tube branches. The amount of debris and firm attachment of the debris particles to the tube in the reinforced section made it impossible to mount samples of intact reinforced segments for microscopic examination or to remove the debris without disruption of the inner lining biofilm. Therefore, only the unreinforced sections

of the tubes were analyzed in this study. The tube caps (apex of the reinforced section) were cut off at the sediment surface and the tubes exhumed until approximately 20-25 cm of the unreinforced portions were exposed. The length of the reinforced portion of each tube was measured and the approximate distance of the upper end of the unreinforced section from the sediment surface determined. From each tube a 20 cm sample (the deepest 2 cm of the reinforced and the first 18 cm of the unreinforced) was removed and further dissected into two 10 cm segments, designated segment A and B (Figure 1). These segments were selected to permit examination of the biofilm at close proximity to the tube inlet and at greater distance from it. Segment A consisted of 2 cm of the reinforced and the first 8 cm of the unreinforced. Segment B was the remaining 10 cm of the unreinforced tube sample. The 2 cm reinforced end of segment A and the first 2 cm of segment B permitted convenient handling of the tube samples without disruption of the biofilm in the remaining 8 cm segments.

Five *D. cuprea* tubes were collected in February 1997. The water and sediment temperatures at the time of collection were 20° C and 19° C, respectively. The samples were placed in 0.2 µm filtered 2.5% formalin, transported to Columbia, SC, and stored at 4° C in the dark for no more than one week prior to analysis. Five additional *D. cuprea* tubes were collected in October 1997. The water temperature was 26° C and the sediment temperature was 25° C at that time. Tubes were handled as described above, but with the following modifications: (1) only segment A for each tube was collected and (2) tube samples were not formalin fixed. These samples were transported to Columbia, SC and held in a recirculating sea water tank overnight.

Sample preparation and staining procedures. Each of the ten February 1997 tube segments was secured onto a glass microscope slide with rubber bands approximately 5 cm apart. The 2 cm ends designated for handling were then removed. The portion of the 8 cm segment between the two rubber bands was cut longitudinally and unrolled with the inner tube surface facing up. These samples were stained for enumeration and measurement of total cells and microcolonies.

SYTOX Green was selected as the primary fluorescent stain after substantial background fluorescence problems were encountered with acridine orange and fluorescein isothiocyanate. DAPI (4,6-diamidino-2-phenylindole) was not tested since the excitation wavelength needed for this dye could not be obtained with our confocal microscope system. Fluorescence background from SYTOX Green, SYTO-9, and propidium iodide was quite low and permitted detailed assessment of cell distributions and appearances. One hundred μL of a 12.5 μM solution of SYTOX Green (Molecular Probes, Inc., Eugene, OR) were added directly onto the inner surface and the sample incubated at room temperature in the dark for 5 minutes. SYTOX Green penetrates only fixed cells (Roth et al. 1997), complexing with DNA. The stain-DNA complex fluoresces green when excited (excitation/emission: 504 nm/523 nm). After incubation, a solution of 1,4-diazobicyclo[2,2,2]octane:glycerol (1:3) (Sigma, St. Louis, MO) was added to reduce photobleaching. A 22 mm x 40 mm coverslip was taped down on top of the sample, holding it flat. The unfixed October 1997 tube segments were mounted as described above and stained for the enumeration of active and inactive cells (Lawrence et al. 1997). Metabolically active bacteria create a proton gradient across their plasma

membrane through active transport of protons out of the cell. This electrochemical gradient, called the proton motive force, or membrane potential, provides a source of energy that can be used to drive ATP synthesis. SYTO-9 (excitation/emission: 488 nm/509 nm; Molecular Probes, Inc., Eugene, OR) only penetrates cells having membrane potential (Lebaron et al. 1998) and fluoresces green upon excitation. These cells are considered to be potentially active. Propidium iodide (excitation/emission: 535 nm/617 nm; Molecular Probes, Inc., Eugene, OR) only penetrates cells lacking membrane potential (Kaneshiro et al. 1993) and fluoresces red upon excitation. These cells are considered to be inactive. One hundred μL of a 50 μM SYTO-9, 149 μM propidium iodide staining solution were added to the samples, which were incubated and mounted as described above.

Confocal scanning laser microscopy. A Bio-Rad MRC – 1000 Laser Scanning Confocal Microscope (Hercules, CA) equipped with a krypton/argon ion laser was used to produce fluorescence images of the tube lining biofilms. Confocal microscopy allows optical sectioning of the biofilm using an adjustable z-axis stepping motor. At set successive intervals, the tunable laser (set to the appropriate excitation wavelength) is scanned over the sample and excites fluorescent dye complexes in a specific focal plane, allowing detection of stained cells at that specific depth (z) in the biofilm. Data were collected at 1 μm depth intervals in the biofilm until the tube wall was encountered, providing a complete z-profile of images from the top of the biofilm to the tube wall. The laser does not penetrate below the tube wall inner surface, and no fluorescence is observable below that depth (Figure 1).

Two z-profiles were taken at each of five sites in each of the SYTOX Green stained tube segments. One profile of each pair was collected at 1000X magnification to allow determination of single cell distribution, the other at 400X magnification for determination of microcolony distribution. The first site in each tube segment was approximately 2.5 cm from the top of the segment (site 1), with successive sites (sites 2-5) at 5 mm intervals along the length of the segment. The dimensions of the fields of view were dependent on the objective used (1000X: 114 x 76 μm, 400X: 288 x 192 μm). Although data sets for single cell and microcolony distributions were collected at approximately the same sites, each is considered to be an independent sample due to microscale differences in biofilm surface texture and the difference in the areas analyzed using 1000X and 400X magification.

Profiles were also collected at five sites at 1000X magnification in each of the activity stained samples. A split spectral line (488 nm and 568 nm) was used to excite both SYTO-9 and propidium iodide in order to visualize the potentially active (green) and non-active (red) cells simultaneously. Data were not collected on microcolonies in segments stained to determine potentially active bacteria due to the bright fluorescence of SYTO-9, which tended to overwhelm the fluorescence of propidium iodide in multicellular aggregates.

Data collection. Data collected at 1 μm depth intervals in the biofilm to determine the distribution of single bacterial cells (February 1997 tubes) were compiled into a series of

5 μm intervals (i.e. 0-5 μm, 6-10 μm, 11-15 μm, etc.) and the number of cells present in each interval counted. A total of 50 sites were examined for single cell distribution within the five tubes, but data for one site in one tube (tube 1, segment A, site 1) were lost due to faulty digital storage. In order to avoid duplicate counting of cells that were at the border of two adjacent 5 μm intervals, each interval image (except 0-5 μm) of a sequential pair of intervals was highlighted in a different color (red or green) and the two images were overlapped. Cells present in both intervals were indicated by yellow highlighting and were counted only in the first of the two intervals. Bacterial cells present in multicellular aggregates of more than 5 cells were not counted in these profiles. Lengths and widths of 10 arbitrarily selected cells were determined for each depth interval by optical magnification of collected images and measurement using calipers. If less than 10 cells were present in an interval, then each cell was measured. Mean cell size (average biovolume of a single cell) for each interval was calculated from the length and width measurements determined for single cells (Norland 1993). The total biovolume of single cells for each 5 μm interval was calculated by multiplying the number of cells in that interval by the mean cell size for that interval.

Fifty sites were analyzed for the distribution of all types of multicellular aggregates. All multicellular aggregates, whether tightly packed and representing relatively high densities of cells, or loosely arranged, with relatively few cells, were designated as microcolonies. For each site, the 1 μm images collected at 400X magnification were compiled in 3 μm intervals. Some sites did not contain microcolonies. In some others, profiles were not completely perpendicular to the tube

wall, prohibiting accurate measurement of depths in the biofilm. A total of 46 sites yielded useful data on microcolony distributions and sizes. Microcolony cross sectional area in each of the 3 μm intervals was measured using MorphoSys (Meacham and Duncan 1991). Biovolumes of the microcolonies were estimated by multiplying the microcolony cross sectional areas in the sequential 3 μm intervals by the total depth of biofilm through which the colonies extended. No attempt was made to differentiate biovolume occupied by cells from that containing only exopolymeric materials. Due to microscale differences in the sites at which single cell and microcolony data were collected, total biovolume of bacteria, which would include all cells regardless of differing modes of growth, were not calculated.

Depth intervals (5 μm) of each profile at the 5 sites in each of the tube segments stained to determine potentially active bacteria were compiled as described above and the number of potentially active cells and non-viable or inactive cells in each of the resulting 5 μm depth intervals were counted. Duplicate counting of cells located at the border of two adjacent intervals was avoided by aligning the two intervals side by side and comparing cell placement in the field of view. One arbitrarily selected profile from each activity stained tube segment was used for determination of average sizes of active and inactive cells (tube 1, site 1; tube 2, site 1; tube 3, site 5; tube 4, site 2; tube 5, site 3) as described above. Lengths and widths of all potentially active and inactive cells were measured and mean cell sizes calculated for each of the 5 μm intervals in these profiles as described above.

Statistical analyses: The SAS System for Windows (version 6.12, SAS Institute, Inc., Cary, NC, USA) was used to perform all statistical analyses. Nested Analysis of Variance was used to determine significant differences in cell numbers, cell size, and biovolume among tubes, among segments, and among sites for data collected from *D. cuprea* tubes stained with SYTOX Green. Regression analysis was used to evaluate relationships between cell numbers, mean cell size, or biovolume, and depth in the biofilm for all sets of tube segments. Cell size variance was modeled using the gamma distribution with Generalized Linear Model (GLIM), using Generalized Estimating Equations (GEE) to accommodate the nested design. All data were tested for normality and statistical tests were performed using a significance level of $\alpha = 0.05$.

RESULTS AND DISCUSSION

Bacterial single cell distributions and sizes

Confocal microscopy revealed that the tubes of *Diopatra cuprea* supported substantial biofilms containing abundant bacteria occurring as single cells and in microcolonial formations. The thickness of *D. cuprea* tube biofilm ranged from 30 μm to 110 μm, with an average thickness of 60 μm. The quantity of individual bacterial cells at a given site ranged from 1.38×10^8 to 1.33×10^9 cells•cm^{-3} (mean = 5.61×10^8 cells•cm^{-3}, Figure 2A). Nested analysis of variance revealed that cell numbers differed significantly from site to site (df 8, 31; $F = 3.00$; $p \leq 0.02$), but not among tubes (df 4,4; $F = 3.14$; $p \geq 0.14$) or between segments A and B (df 4,8; $F = 1.01$; $p \geq 0.45$). There was no consistent pattern of cell distribution within the tube lining biofilm (Figure 3).

Twenty-five of the 49 sites had highest cell numbers within 10 μm of the biofilm surface. Twenty-three had additional subsurface peaks in cell numbers. Cell numbers decreased significantly (regression analysis, $p < 0.05$ in all cases) with increasing depth in the biofilm at 28 of the 49 sites, but the remaining sites showed no significant changes with depth.

Unlike cell numbers, mean bacterial cell sizes did change with depth below the sediment surface. Cell sizes at different sites in the tube segments ranged from 0.032 μm^3 to 0.285 μm^3 (grand average: 0.085 μm^3, Figure 2B). Nested analysis of variance revealed significant differences in mean cell size between segments A and B (df 4,8; $F = 4.93$; $p \leq 0.03$), with cells in segment B averaging larger than those in segment A. No significant differences in mean cell size were found among tubes (df 4,4; $F = 0.60$; $p \geq 0.68$) or sites (df 8,31; $F = 1.19$; $p \geq 0.3$). Based on *D. cuprea* behavior and bacterial stress responses, this trend is quite different from what would be expected. *D. cuprea* spends most of its time in the upper portion of the tube near the sediment surface and irrigation of the tube is frequent but not continuous. At the depths of the tube sites examined (10 cm to 36 cm below the sediment surface), the only oxygen available to the microbiota and a substantial portion of the nutrient inputs are provided by host irrigation. Consequently, sites at greater depths should experience greater oxygen and/or nutrient limitation due to the lesser impact of irrigation. Bacteria in nature that are severely nutrient limited are typically smaller than their more resource-sufficient counterparts (Chesbro et al. 1990, Kaprelyants et al. 1993, Kjelleberg et al. 1983). If cells located

deeper in the tube were oxygen and/or nutrient limited they should have been smaller than those at shallower depths, but that was not the case.

There was also a clear pattern in the distribution of bacterial cell size with depth in the burrow lining biofilm (Figure 3). The largest mean cell sizes were found in intervals within 10 μm of the biofilm surface at 32 of the 49 sites. Nineteen sites had subsurface peaks in cell size. Almost all sites (42 out of 49) showed significant decreases in mean cell size (regression analysis, $p < 0.05$ in all cases) and of variance in cell size ($E = -0.0005$; $SE = 0.0002$; $Z = -1.906$; $p \leq 0.01$) with increasing depth into the biofilm. This trend may have been due to nutrient or oxygen limitation at the base of the biofilm.

The biovolume of single cells at a given site, a function of the grand average of cell sizes (i.e. average of mean cell sizes for all intervals at that site) and cell numbers, ranged from 7.26×10^6 to 3.53×10^8 $\mu m^3 \bullet cm^{-3}$ (mean = 5.33×10^7 $\mu m^3 \bullet cm^{-3}$, Figure 2C). Nested analysis of variance showed that biovolume differed significantly among sites (df 8,31; $F = 2.39$; $p \leq 0.04$) but not between segments A and B (df 4,8; $F = 2.06$; $p \geq 0.17$) or among tubes (df 4,4; $F = 0.95$; $p \geq 0.51$). The highest biovolumes in 24 of 49 sites were within 10 μm of the biofilm surface while 12 sites had subsurface biovolume peaks. There was a significant relationship between biovolume and depth in the biofilm at 34 of 49 sites, and biovolume decreased with increasing depth in the biofilm in at least half of the sites in each tube (Figure 2).

Microcolony distribution

Microcolonies covered a broad range of sizes and were found throughout the length of the *D. cuprea* tube and at all depths within the biofilm. The number of microcolonies at a given site ranged from 1 to 31 (mean = 5) and these formations were located at various depths throughout the biofilm. Microcolony biovolume ranged from 16 μm^3 to 2.5 x 10^5 μm^3 (mean = 1.28 x 10^4 μm^3). Nested analysis of variance revealed that the microcolony biovolumes did not differ significantly among sites (df 8,28; $F = 1.55$; $p \geq 0.18$), between segments A and B (df 4,8; $F = 1.83$; $p \geq 0.21$), or among tubes (df 4,4; $F = 1.96$; $p \geq 0.26$). The structures of microcolonies varied from very tightly organized formations to loose aggregations of cells and expolymers. The potential of these structures to facilitate interactions among different bacterial species (Paerl and Pinckney 1996) is clear and their formation may be very important to the overall activities of the biofilm.

Potentially active vs. inactive cells

D. cuprea tubes were also stained to permit determination of the proportions of cells that were intact and potentially active versus those lacking membrane potential and thus presumably inactive (Lawrence et al. 1997). The total number of cells per site in segments stained to determine bacterial activity ranged from 2.62 x 10^8 to 1.71 x 10^9 cells $\bullet cm^{-3}$ (mean = 6.11 x 10^8 $\bullet cm^{-3}$). The proportion of total cells that were potentially active was quite high (Figure 4), ranging from 0.46 to 0.85 (mean = 0.68), and did not

significantly differ among sites (df 4,16; $F = 1.33$; $p \geq 0.29$). Potentially active cells were observed at all depths within the biofilm (Figure 5) and the proportion of cells that were potentially active was similar at all depths at 19 of the 25 sites. The proportion of active cells increased with increasing depth in the biofilm at three sites and decreased with increasing depth at the remaining three sites ($p < 0.05$ in all cases). The abundance of potentially active cells was not surprising since previous studies have shown that infaunal burrows are sites of intense microbial activity and contain substantial amounts of viable microbial biomass (Aller 1980, Aller and Yingst, 1978, Dobbs and Guckert 1988, Steward et al. 1996). What was surprising was that cells at depth in the biofilm and at sites far below the sediment surface appear to be as capable of activity as those near the biofilm surface and at sites near the sediment surface.

Sizes of potentially active and inactive cells were also measured at one site in each of the five tube segments. The average size of potentially active cells ranged from 0.19 μm^3 to 0.42 μm^3 (grand mean = 0.3 μm^3) and was significantly larger than that of inactive cells (range: 0.15 μm^3 to 0.28 μm^3, grand mean = 0.18 μm^3) across all five tubes (df 4; $T = 4.37$; $p \leq 0.01$) (Figure 6). There was no general pattern in the distribution of potentially active or inactive mean cell sizes in relation to the depth in the biofilm (Figure 7). The variance of potentially active cell size significantly decreased with increasing depth in the biofilm ($E = -0.0017$; $SE = 0.0006$; $Z = -2.945$; $p \leq 0.01$) while the variance of inactive cell size increased with depth ($E = 0.0005$; $SE = 0.0004$; $Z = -1.416$; $p \leq 0.01$). The observed size differences between potentially active and inactive cells were

consistent with reports of stressed or starved cells averaging smaller than actively growing cells of the same species (reviewed in Kjelleberg et al. 1987).

Comparisons were also made between mean cell numbers and sizes in the A segments of tubes collected in October 1997 and February 1997. There was no significant difference in the mean number of cells per tube between the two sets (df 1,8; $F = 0.31$; $p \geq 0.50$). However, there was a difference in mean cell size. Mean cell sizes in tubes collected in October 1997 for activity staining were significantly larger, 0.18 – 0.38 μm^3, than those in tubes collected in February 1997, 0.058 – 0.09 μm^3 (df 1,8; $F = 0.093$; $p \leq 0.01$). One clear difference between the February and October samples was formaldehyde fixation of the February samples. Turley and Hughes (1992) reported about 10% reduction in cell size (estimated from digitized cell images) in fixed samples stored for 39 to 53 days, but provided no data for shorter storage times. Troussellier et al. (1995), using flow cytometric light scatter techniques, found no measurable changes in cell structure or morphology in samples fixed for a much shorter time period (24 h). The short times (≤1 week) our fixed samples were stored prior to analysis seem unlikely to produce significant cell shrinkage. Even shrinkage comparable to that reported by Turley and Hughes (1992) could not account for the almost three-fold difference in mean cell size we observed between the February and October samples. A more likely explanation for the difference in cell size can be based on the biology of *D. cuprea*. The water temperature in October was warmer than in February and the polychaetes likely irrigated more actively in October (e.g. Mangum and Sassaman 1969). More frequent irrigation during the warmer period would increase the availability of oxygen and nutrients.

Warmer water temperature would also have a positive effect on the bacterial communities, resulting in faster growth and an increase in mean cell size.

The differences in the relationship of mean cell size and depth in the biofilm between the two collection dates could also be a result of irrigation intensity and frequency. In February cells became smaller and more uniform in size with increasing depth in the biofilm. This trend was not observed in tubes collected in October and could be due to oxygen and nutrient limitation of microorganisms located deeper in the biofilm.

Recent studies of many laboratory-cultivated biofilms have revealed channels of low-density-exopolymer throughout the material (e.g. Stewart et al. 1993, Stoodley et al. 1994, Wolfaardt et al. 1994). These channels are thought to be essential for nutrient transport to organisms deep within the biofilm (Costerton et al. 1995, Lawrence et al. 1994) and can be revealed through staining with fluorescently tagged lectins, which bind specifically to the biofilm polysaccharides. Staining with fluorescein isothiocyanate-labeled concanavalin A (Sigma, St. Louis, MO), which selectively binds α-mannopyranosyl and α-glucopyranosyl residues in polysaccharides, revealed no channels within the *D. cuprea* tube biofilm (data not shown). *D. cuprea* deposits many layers of mucus over time and cells that are on the surface of the tube lining eventually become embedded within the tube matrix. Any channels that might arise could be filled with worm mucus on the next cycle of polymer deposition. However, channels may not be required for active microbial metabolism throughout the tube lining biofilm. Aller (1983) suggested that the tube linings of macro-infaunal organisms could be considered to be highly hydrated porous membranes (Aller 1983). Diffusion of small molecules through

the tube (including the biofilm) would not be hindered by such materials and thus activity of bacteria at depth in the biofilm could be supported.

The *D. cuprea* tube supports an abundant and varied microbial community that contains an unusually high proportion of potentially active cells. These findings are consistent with the high levels of microbial biomass and activity reported for various infaunal burrows and tubes. The trends observed in cell size distributions are very intriguing in that they may reflect the nutritional and/or stress regimes the organisms experience in response to irrigation of the tube by *D. cuprea*. Manipulative experiments exploring the impact of tube irrigation on biofilm microbiota and molecular biological characterization of these organisms are ongoing.

Acknowledgements

We gratefully acknowledge John Kaigler for drawing Figure 1, Holms Finch and Sarah Woodin for their assistance with statistical analysis of data, Sarah Woodin for information on the lifestyle and habits of *Diopatra cuprea*, and Courtney Richmond for her help with MorphoSys. We would also like to thank Bob Price (IMAF, Univ. South Carolina Medical School) for his guidance in the use of the confocal microscope.

This research was supported by grant number N000149610403 from the United States Office of Naval Research to C.R.L.

References

Allen DM, Service SK, Ogburn-Matthews MV (1992) Factors influencing the collection efficiency of estuarine fishes. Trans Amer Fish Soc 121:234-244

Aller JY, Aller RC (1986) Evidence for localized enhancement of biological activity associated with tube and burrow structures in deep-sea sediments at the HEBBLE site, western North Atlantic. Deep Sea Res 33:755-790

Aller RC (1980) Quantifying solute distributions in the bioturbated zone of marine sediments by defining an average microenvironment. Geochim Cosmochim Acta 44:1955-1965

Aller RC (1983) The importance of the diffusive permeability of animal burrow linings in determining marine sediment chemistry. J Mar Res 41:299-322

Aller RC (1988) Benthic fauna and biogeochemical processes in marine sediments: the role of burrow structures. In: Blackburn TH, Sorensen J (eds) Nitrogen cycling in coastal marine environments. Wiley, Chichester, UK, p. 301-338

Aller RC, Yingst JY (1978) Biogeochemistry of tube dwellings: a study of the sedentary polychaete *Amphitrite ornata* (Leidy). J Mar Res 36:201-254

Binnerup SJ, Jensen K, Revsbech NP, Jensen MH, Sorensen J (1992) Denitrification, dissimilatory reduction of nitrate to ammonium, and nitrification in a bioturbated estuarine sediment as measured with ^{15}N and microsensor techniques. Appl Environ Microbiol 58:303-313

Boudreau BP, Marinelli RL (1994) A modelling study of discontinuous biological irrigation. J Mar Res 52:947-968

Chesbro W, Arbige M, Eifert R (1990) When nutrient limitation places bacteria in the domains of slow growth: metabolic, morphologic and cell cycle behavior. FEMS Microb Ecol 74:103-120

Costerton JW, Lewandowski Z, Caldwell DE, Korber DR, Lappin-Scott HM (1995) Microbial biofilms. Annu Rev Microbiol 49:711-745

Dobbs FC, Guckert JB (1988) *Callianassa trilobata* (Crustacea:Thalassinidae) influences abundance of meiofauna and biomass, composition, and physiological state of microbial communities within its burrow. Mar Ecol Prog Ser 45:69-79

Fenchel T (1969) The ecology of marine microbenthos. IV. Structure and function of the benthic ecosystem, its chemical and physical factors and the microfauna communities with special reference to the ciliated protozoa. Ophelia 6:1-182

Findlay RH, White DC (1983) The effects of feeding by the sand dollar *Mellita quinquiesperforata* (Leske) on the benthic microbial community. J Exp Mar Biol Ecol 72:25-41

Findlay RH, White DC (1984) *In situ* determination of metabolic activity in aquatic environments. Microbiol Sci 1:90-95

Findlay RH, Trexler MB, White DC (1990) Response of a benthic microbial community to biotic disturbance. Mar Ecol Prog Ser 62:135-148

Grant J (1983) The relative magnitude of biological and physical sediment reworking in an intertidal community. J Mar Res 41:673-689

Kaneshiro E, Wyder MA, Wu Y, Cushion MT (1993) Reliability of calcein acetoxy methyl ester and ethidium homodimer or propidium iodide for viability assessment of microbes. J. Microbiol. Methods 17:1-16

Kaprelyants AS, Gottschal JC, Kell DB (1993) Dormancy in non-sporulating bacteria. FEMS Microbiol Rev 104:271-286

Kjelleberg S, Hermansson M, Mårdén P, Jones GW (1987) The transient phase between growth and nongrowth of heterotrophic bacteria, with emphasis on the marine environment. Annu Rev Microbiol 41:25-49

Krantzberg G (1985) The influence of bioturbation on physical, chemical and biological parameters in aquatic environments: a review. Environ Pollut 39:99-122

Kristensen E, Jensen MH, Aller RC (1991) Direct measurement of dissolved inorganic nitrogen exchange and denitrification in individual polychaete (*Nereis virens*) burrows. J Mar Res 49:355-377

Kristensen E, Jensen MH, Andersen TK (1985) The impact of polychaete (*Nereis virens* Sars) burrows on nitrification and nitrate reduction in estuarine sediments. J Exp Mar Biol Ecol 85:75-91

Lawrence JR, Korber DR, Wolfaardt GM, Caldwell DE (1997) Analytical imaging and microscopy techniques. In: Hurst CJ, Knudsen GR, McInerney MJ, Stetzenbach LD, Walter MV (ed) Manual of environmental microbiology. ASM Press, Washington, DC, p 29-51

Lawrence JR, Wolfaardt GM, Korber DR (1994) Determination of diffusion coefficients in biofilms by confocal laser microscopy. Appl Environ Microbiol 60:1166-1173

Lebaron P, Parthuisot N, Catala P (1998) Comparison of blue nucleic acid dyes for flow cytometric enumeration of bacteria in aquatic systems. Appl Environ Microbiol 64:1725-1730

Lovell CR, Piceno Y (1994) Purification of DNA from estuarine sediments. J Microbiol Meth 20:161-174

Mangum C, Sassaman C (1969) Temperature sensitivity of active and inactive metabolism in a polychaetous annelid. Comp Biochem Physiol 30:111-116

Marinelli RL, Boudreau BP (1996) An experimental and modeling study of pH and related solutes in an irrigated anoxic coastal sediment. J Mar Res 54:939-966

Meacham C, Duncan T (1991) Morphosys. Version 1.29. University Herbarium, Univerisity of California, Berkley, California.

Myers AC (1972) Tube-worm-sediment relationships of *Diopatra cuprea* (Polychaeta:Onuphidae) Mar Biol 17:350-356

Norland S (1993) The relationship between biomass and volume of bacteria. In: Kemp PF, Sherr BF, Sherr EB, Cole JJ (eds) Handbook of methods in aquatic microbial ecology. Lewis Publishers, Boca Raton, FL, p 303-307

Novitsky JA (1983) Heterotrophic activity throughout a vertical profile of seawater and sediment in Halifax Harbor, Canada. Appl Environ Microbiol 45:1753-1760

Novitsky JA, Karl DM (1986) Characterization of microbial activity in the surface layers of a coastal sub-tropical sediment. Mar Ecol Prog Ser 28:49-55

Paerl HW, Pinckney JL (1996) A mini-review of microbial consortia: their roles in aquatic production and biogeochemical cycling. Microb Ecol 31:225-247

Revsbech NP, Jorgensen BB (1986) Microelectrodes: their use in microbial ecology. Adv Microb Ecol 9:293-352

Roth BL, Poot M, Yue ST, Millard PJ (1997) Bacterial viability and antibiotic susceptibility testing with SYTOX Green nucleic acid stain. Appl Environ Microbiol 63:2421-2431

SAS Institute Inc (1997) SAS/STAT© Software: changes and enhancements through release 6.12. Cary, NC: SAS Institute Inc., 1167 pp.

Steward CC, Nold SC, Ringelberg DB, White DC, Lovell CR (1996) Microbial biomass and community structures in the burrows of bromophenol producing and non-producing marine worms and surrounding sediments. Mar Ecol Prog Ser 133:149-165

Stewart PS, Peyton BM, Drury WJ, Murga R (1993) Quantitative observations of heterogeneities in *Pseudomonas aeruginosa* biofilms. Appl Environ Microbiol 59:327-329

Stoodley P, deBeer D, Lewandowski Z (1994) Liquid flow in biofilm systems. Appl Environ Microbiol 60:2711-2716

Troussellier M, Courties C, Zettelmaier S (1995) Flow cytometric analysis of coastal lagoon bacterioplankton and picophytoplankton: fixation and storage effects. Estuar Coast Shelf Sci 40:621-633

Turley CM, Hughes DJ (1992) Effects of storage on direct estimates of bacterial numbers of preserved seawater samples. Deep Sea Res 39:375-394

Wolfaardt GM, Lawrence JR, Robarts RD, Caldwell SJ, Caldwell DE (1994) Multicellular organization in a degradative biofilm community. Appl Environ Microbiol 60:434-446

Yingst JY, Rhoads DC (1980) The role of bioturbation in the enhancement of bacterial growth rates in marine sediments. In: Tenore KR, Coull BC (eds) Marine Benthic Dynamics. Univ. South Carolina Press, Columbia, SC, p 407-421

Figure Legends

Figure 1. Schematic diagram of *Diopatra cuprea* tube structure and the sampling procedure used to determine distributions of bacteria in *D. cuprea* tube lining biofilms. For each tube, two 8 cm segments of the unreinforced portion (segment A and B) were collected. In each of the segments, five sites (1-5) were examined. At each site, confocal images were collected at 1 μm depth intervals from the surface of the biofilm to the tube wall.

Figure 2. Cells per cm^3 (A), mean cell size (B), and biovolume (cell numbers multiplied by mean cell size at each site) (C) in *Diopatra cuprea* tube lining biofilms. Mean (± SD) is shown for each of the five sites within each segment across all 5 tubes (n = 5 except for segment A, site 1, where n = 4).

Figure 3. Distribution of cell numbers (bars), mean cell size (± SD, n = 1-10) (closed circles) and biovolume (cell numbers multiplied by mean cell size per 5 μm interval) (open triangles) with increasing depth into *Diopatra cuprea* tube lining biofilm for sites 1 (A), 2 (B), 3 (C), 4 (D) and 5 (E) in segment A of tube 2.

Figure 4. Total (black bars) and potentially active (open bars) cells per cm^3 for each site in segment A of *Diopatra cuprea* tube lining biofilms. Mean (± SD) is shown for each site for 5 tubes.

Figure 5. Total (black bars) and potentially active (open bars) cells per cm^3 in segment A of *Diopatra cuprea* tube lining biofilms. Mean (± SD) at each depth in the biofilm, across all sites, is shown. The number of samples varies from 1 to 25 at different depths in the biofilm due to differences in biofilm thickness at different sites.

Figure 6. Potentially active (closed circles) and inactive (open triangles) cell sizes in *Diopatra cuprea* tube lining biofilms. Mean (± SD) is shown for one site in each tube. Sample size (n) for potentially active cells ranges from 43 to 94; sample size (n) for inactive cells ranges from 33 to 79.

Figure 7. Mean potentially active (closed circles) and inactive (open triangles) cell sizes in *Diopatra cuprea* tube lining biofilms. Means (± SD) at each depth in the biofilm, across all five sites, is shown. The number of samples at a given depth in the biofilm varies due to differences in biofilm thickness (n = 1 – 5).

Figure 1

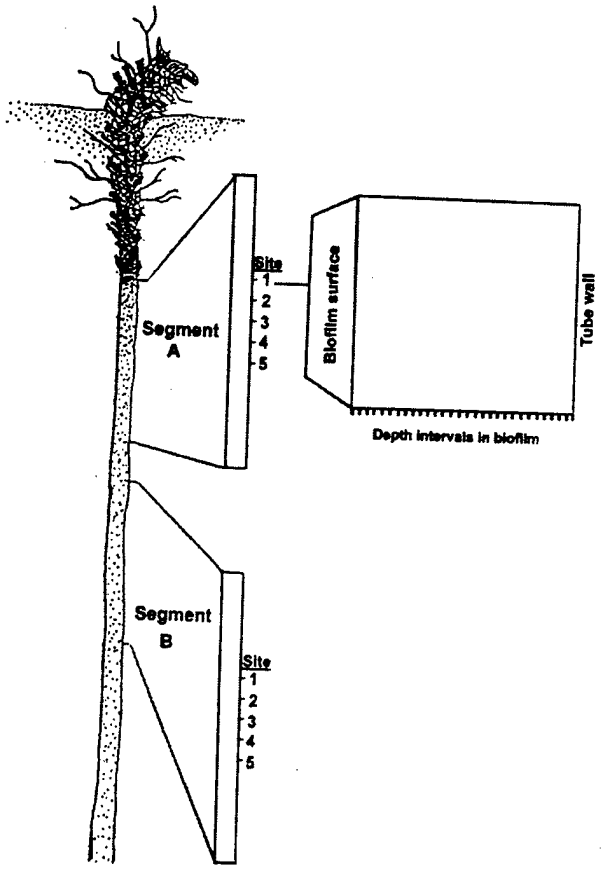
Site
1
2
3
4
5
Segment
A
Biofilm surface
Tube wall
Depth intervals in biofilm
Segment
B
Site
1
2
3
4
5

Figure 2

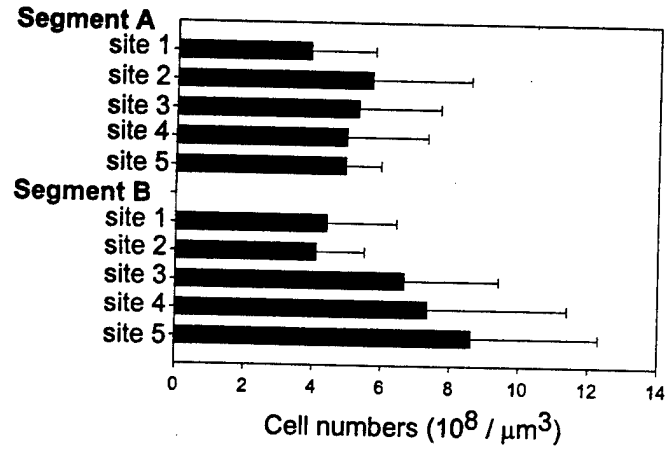
Segment A
site 1
site 2
site 3
site 4
site 5
Segment B
site 1
site 2
site 3
site 4
site 5
0
2
4
6
8
10
12
14
Cell numbers (10^8 / μm^3)

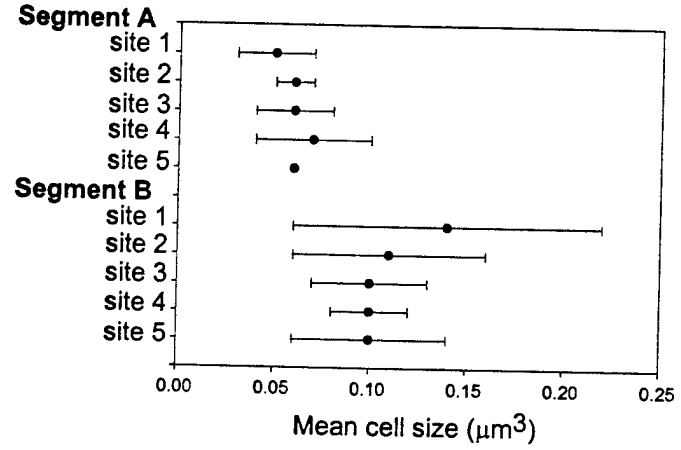
Segment A
site 1
site 2
site 3
site 4
site 5
Segment B
site 1
site 2
site 3
site 4
site 5
0.00
0.05
0.10
0.15
0.20
0.25
Mean cell size (μm^3)

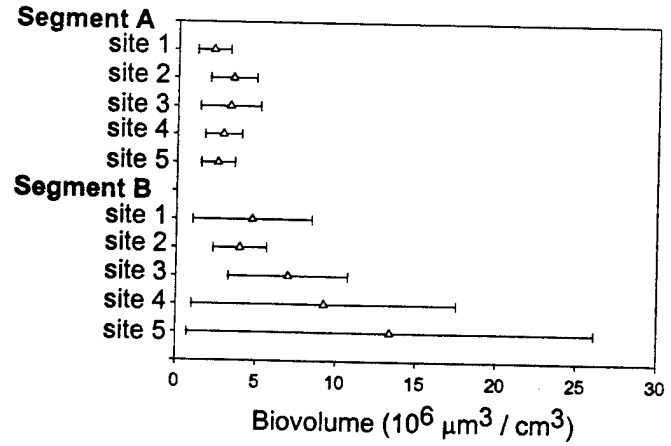
Segment A
site 1
site 2
site 3
site 4
site 5
Segment B
site 1
site 2
site 3
site 4
site 5
0
5
10
15
20
25
30
Biovolume (10^6 μm^3 / cm^3)

Figure 3

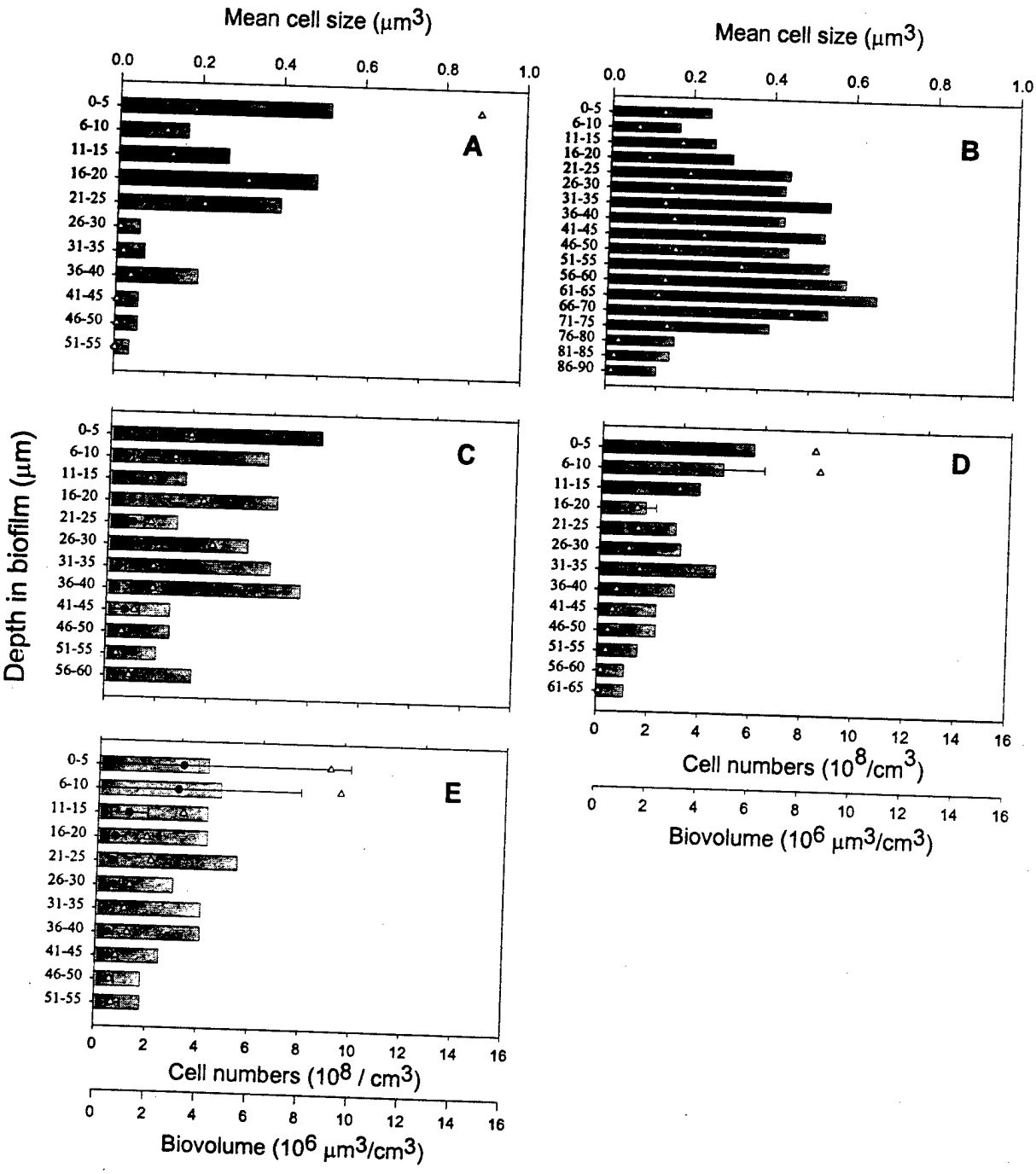
Mean cell size (μm3)
0.0
0.2
0.4
0.6
0.8
1.0
0-5
6-10
11-15
16-20
21-25
26-30
31-35
36-40
41-45
46-50
51-55
A
Mean cell size (μm3)
0.0
0.2
0.4
0.6
0.8
1.0
0-5
6-10
11-15
16-20
21-25
26-30
31-35
36-40
41-45
46-50
51-55
56-60
61-65
66-70
71-75
76-80
81-85
86-90
B
Depth in biofilm (μm)
0-5
6-10
11-15
16-20
21-25
26-30
31-35
36-40
41-45
46-50
51-55
56-60
C
0-5
6-10
11-15
16-20
21-25
26-30
31-35
36-40
41-45
46-50
51-55
56-60
61-65
D
0
2
4
6
8
10
12
14
16
Cell numbers (10^8/cm^3)
Biovolume (10^6 μm3/cm3)
0-5
6-10
11-15
16-20
21-25
26-30
31-35
36-40
41-45
46-50
51-55
E
0
2
4
6
8
10
12
14
16
Cell numbers (10^8 / cm3)
Biovolume (10^6 μm3/cm3)

Figure 4

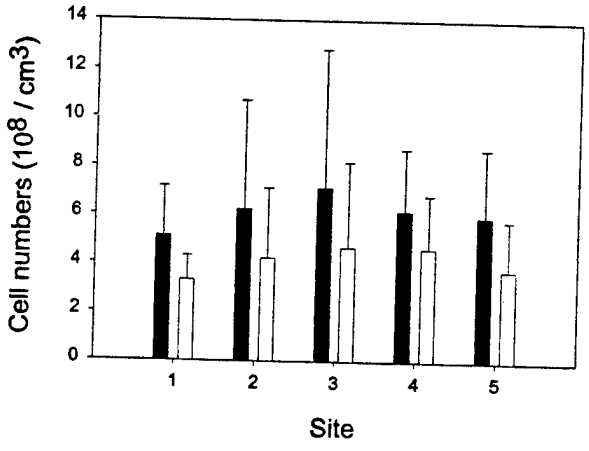

Figure 5

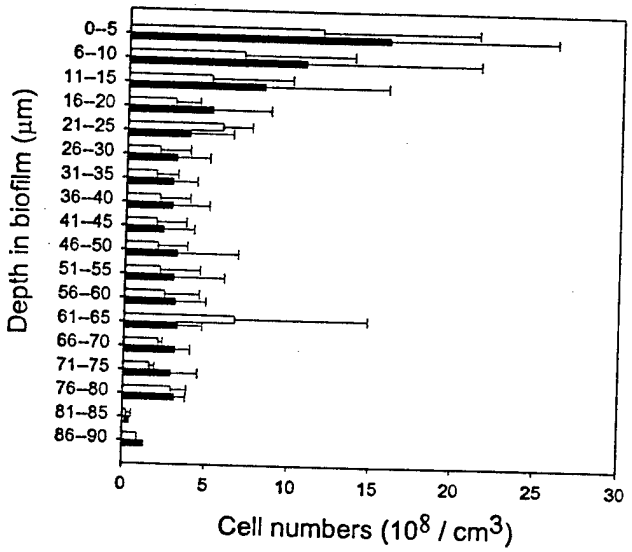
Depth in biofilm (µm)
0–5
6–10
11–15
16–20
21–25
26–30
31–35
36–40
41–45
46–50
51–55
56–60
61–65
66–70
71–75
76–80
81–85
86–90
0
5
10
15
20
25
30
Cell numbers (10^8 / cm^3)

Figure 6

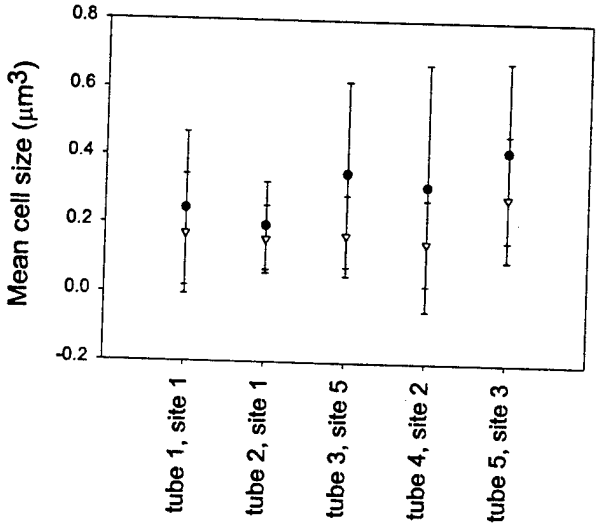
Mean cell size (µm3)
0.8
0.6
0.4
0.2
0.0
-0.2
tube 1, site 1
tube 2, site 1
tube 3, site 5
tube 4, site 2
tube 5, site 3

Figure 7

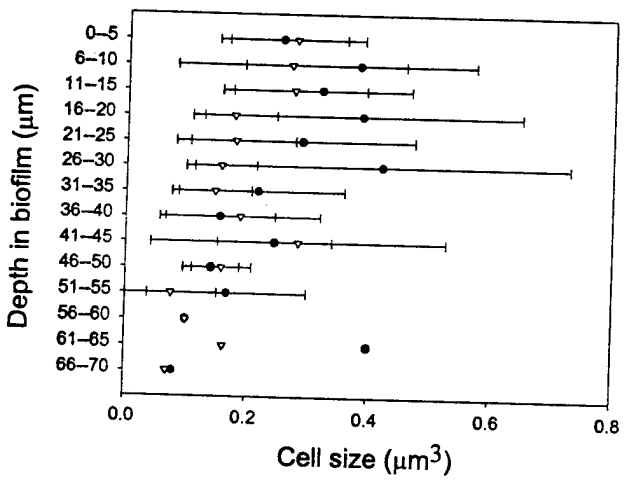
Depth in biofilm (µm)
0–5
6–10
11–15
16–20
21–25
26–30
31–35
36–40
41–45
46–50
51–55
56–60
61–65
66–70
0.0
0.2
0.4
0.6
0.8
Cell size (µm³)

Reductively debrominating strains of *Propionigenium maris* from burrows of bromophenol producing marine infauna

Jamey Watson[1], George Y. Matsui[1], Juergen Wiegel[2], Frederick A. Rainey[3,4], and Charles R. Lovell[1*]

[1]Department of Biological Sciences
University of South Carolina
Columbia, SC 29208

[2]Department of Microbiology
University of Georgia
Athens, GA 30602

[3]DSMZ-Braunschweig
Germany, D-38124

[4]Present address: Department of Biological Sciences, Louisiana State University, Baton Rouge, LA 70808

[*]Corresponding author phone: (803)777-7036
FAX: (803)777-4002
Email: lovell@biol.sc.edu

Running title: Debrominating *Propionigenium maris* strains

Key words: Reductive dehalogenation - bromophenols - marine sediments - infaunal burrows – *Propionigenium*

Subject category: New Taxa, Gram-positive bacteria

Abbreviations: TBP – 2,4,6-tribromophenol

SUMMARY

Two novel strains of *Propionigenium maris* able to reductively debrominate 2,4,6-tribromophenol (TBP) to monobromophenols were isolated from marine hemichordate and polychaete burrows. These two strains, DSL-1 and ML-1, were anaerobic, nonmotile rods that stained Gram negative and required 0.05% yeast extract for growth. Strain DSL-1 fermented pyruvate and succinate to butyrate and strain ML-1 fermented glucose and succinate primarily to propionate. No inorganic terminal electron acceptors were identified. The pH and temperature optima for growth of strain DSL-1 were 7.6 and 30° C; 7.0 and 32° C for strain ML-1 with doubling times of 0.32 h and 0.30 h, respectively. Both strains required 2-3% (w/v) NaCl for optimal growth. Morphological and physiological features, as well as the results of 16S rDNA sequence analysis, showed these to be new strains of *Propionigenium maris*. Because they differ from the *P. maris* type strain (DSM 9537) in a number of respects, including their ability to rapidly debrominate di- and tribromophenols, and in their specific habitats, the species description is amended to include these ecologically important properties.

INTRODUCTION

Biogenic bromoaromatic compounds are broadly distributed in intertidal marine sediments (King, 1986; D. E. Lincoln, K. T. Fielman, R. L. Marinelli, and S. A. Woodin, unpublished data; Steward *et al.*, 1992; Woodin *et al.*, 1987). A variety of infaunal hemichordate and polychaete worms produce bromoaromatic compounds, including but not limited to bromophenols, bromopyrroles, bromoindoles, and bromobenzylalcohols (Fielman *et al.*, 1999; Woodin *et al.*, 1987). These bromometabolites are produced through the action of haloperoxidases (Chen *et al.*, 1991) and reach very high levels in the worm tissues (Fielman & Targett, 1995; Yoon *et al.*, 1994). The highest concentrations of bromometabolites external to the animals are found in sediments lining the animals' burrows (King, 1986; D. E. Lincoln, K. T. Fielman, R. L. Marinelli, and S. A. Woodin, unpublished data). Turnover of bromophenols in shallow marine sediments can be rapid (Steward & Lovell, 1997) and the burrow linings, due to the abundance of carbon cosubstrates and potential electron acceptors, and high levels of bacterial biomass (Steward *et al.*, 1996; Phillips & Lovell, 1999), are expected to be sites of enhanced degradation of bromoaromatic compounds. The microbiota inhabiting these burrow lining biofilms are thus of considerable interest for detailed studies of degradation processes for haloaromatic compounds. Presently little is known about the diversity of species carrying out reductive dehalogenation processes in marine systems.

The large extent of contaminated sediments and the diversity of microenvironments available in coastal marine systems implies the existence of a plethora of haloaromatic degrading

species there. However, although mixed culture and sediment slurry studies of marine haloaromatic degradation are abundantly documented in the literature (e.g. Abrahamsson & Klick, 1991; Allard *et al.,* 1991; Boothe *et al.*, 1997; Genthner *et al.*, 1989; Häggblom &Young, 1990, 1995; King, 1988; Monserrate & Häggblom, 1997; Remberger *et al.*, 1986), and many important degradative reactions are known (see El Fantroussi *et al.,* 1998; Fetzner & Lingens, 1994; Häggblom, 1992; Hale *et al.*, 1994; Janssen *et al.*, 1994; Mohn & Tiedje, 1992 for recent reviews), marine strains highly active against multiply substituted haloaromatics have proven difficult to enrich and isolate into pure culture. This is particularly true of reductively dehalogenating organisms, which can remove halogen atoms from the aromatic ring. This process is crucial in the consortial degradation of multiply substituted haloaromatics since compounds with few substituent halogen atoms, particularly monohalogenated aromatics, are mineralized much more readily than multiply substituted compounds with the same aromatic ring structure (Neilson, 1990, Utkin *et al.*, 1995). No pure culture able to dechlorinate multiply chlorinated chloroaromatic compounds has been reported from marine systems and only one marine strain able to debrominate multiply brominated aromatics has been described to date (Steward *et al.*, 1995). This limited roster of dehalogenators restricts studies of the physiology and biochemistry of reductive dehalogenation in marine microorganisms, a reaction catalyzed by several classes of enzymes differing in structure and in some cases in reaction mechanism (Y. P. Chen, J. Watson , and C. R. Lovell, unpublished data; Holliger *et al.*, 1999, Löffler *et al.*, 1996; Ni *et al.*, 1995; Steward *et al.*, 1995). Here we present the characterization and phylogenetic affiliation of two reductively debrominating marine anaerobe strains of *Propionigenium maris*. We amend the description of this species since the two novel strains are capable of rapid

reductive debromination of tri- and dibromophenols, producing monobromophenols as terminal products, a property not described for the type strain.

MATERIALS AND METHODS

Materials and strains. Bromophenol substrates and standards were obtained from Aldrich Chemical and used without further purification. *Propionigenium maris* (DSM 9537) was obtained from the Deutsche Sammlung von Mikroorganismen. The isolation of strain DSL-1 has been described elsewhere (Steward *et al.*, 1995). Samples for enrichment of strain ML-1 were collected from the North Inlet salt marsh, Georgetown, South Carolina, USA. (30°20'N, 79°10'W). These samples consisted of burrow linings of the capitellid polychaete *Notomastus lobatus*, a common inhabitant of clay rich intertidal mud flats in this system and a well-studied producer of 2,4,6-tribromophenol, 2,4-dibromophenol, and 4-bromophenol (Chen *et al.*, 1991; Lovell *et al.*, 1999; Steward *et al.*, 1992, 1996; Steward & Lovell, 1997; Yoon *et al.*, 1994). The burrow scrapings were transported on ice to Columbia, South Carolina, where enrichment cultures were prepared following previously described methods (Steward *et al.*, 1995). Enrichment media had pH values ranging from 5.5 to 7.5, and all contained 1 mM 2,4,6-tribromophenol (TBP); a concentration comparable to that of total bromophenols in *N. lobatus* burrow linings (D. E. Lincoln, K. T. Fielman, R. L. Marinelli, and S. A. Woodin, unpublished data). These enrichment media also contained acetate, lactate, sodium benzoate, or succinate (40 mM final concentration) as supplemental carbon source. The cultures were incubated in the dark at 32° C. Growth was seen within a few days in all cultures except those containing sodium

benzoate. All growing cultures actively debrominated TBP as assessed using gas chromatography (Stewart *et al.*, 1995). The pH 7.0, succinate supplemented culture had few microscopically distinguishable cell types and was selected for pure culture isolation of debrominators using the agar shake method (Steward *et al.*, 1995). Colonies were visible within one week and were aseptically transferred into fresh succinate medium. This process was repeated four times, with each successive culture checked for homogeneity by phase contrast microscopy. All cultures were homogeneous with respect to cell morphology and were apparently identical to each other. One pure culture from this group was selected arbitrarily and designated strain ML-1.

Growth media. DSL-1: The growth medium was a minor modification of the recipe of Steward *et al.* (1995) and contained the following: ($g \cdot l^{-1}$) KH_2PO_4, 0.2; NH_4Cl, 0.3; KCl, 0.5; $CaCl_2 \cdot 2H_2O$, 0.15; NaCl, 20; $MgCl_2 \cdot 6H_2O$, 3.0; Bacto yeast extract, 0.5; SL-9 trace metal solution (Tschech and Pfennig, 1984), 1 $ml \cdot l^{-1}$. The basal medium was adjusted to pH 5.5 and, after autoclaving, the medium was supplemented with sterile filtered 1 mM 2,4,6-tribromophenol, autoclaved cysteine sulfide (0.0028% cysteine - 0.0028% sodium sulfide, w/v, final concentration), and autoclaved $NaHCO_3$ (50 mM final concentration). In some experiments, a supplemental carbon source (acetate, benzoate, citrate, crotonate, ethanol, fumarate, glucose, lactate, malate, oxalate, propionate, pyruvate, or succinate at 4 - 20 mM final concentration) and/or potential terminal electron acceptor (nitrate, fumarate, and sodium thiosulfate at 5 mM final concentration) were added. Routine cultivation of strain DSL-1 was performed using 20 mM succinate as supplemental carbon source with no added terminal electron acceptor. The

complete medium was adjusted to pH 7.5.

ML-1: The growth medium for strain ML-1 was derived from the DSL-1 medium recipe, substituting 4-(2-hydroxyethyl)-1-piperazineethanesulfonic acid (HEPES, 4.8 $g \cdot l^{-1}$) for the carbonate buffer, and adding Bacto Casitone (1.0 $g \cdot l^{-1}$) as an additional supplement. Routine cultivation employed the ML-1 basal medium supplemented with 40 mM succinate. Culture growth was monitored by direct microscopic counting using a Petroff-Hauser counting chamber.

pH and temperature ranges and NaCl requirements. The pH and temperature ranges for growth of strains DSL-1 and ML-1 were determined in triplicate for cultures growing on succinate supplemented basal media. Optimum pH and NaCl requirement determinations were performed at room temperature for strain DSL-1 and at 32° C for strain ML-1. The pH range tested for strain DSL-1 was from 6.5 through 8.5 and for strain ML-1 from 5.5 through 7.5. The temperature range for growth of strain DSL-1 was determined at pH 7.5 over a range from 10° C through 50° C. The temperature range for strain ML-1 was determined at pH 7.0 and temperatures between 20° C and 40° C were used. Both strains were tested for growth within the ranges specified at five degree temperature intervals. Once the approximate temperature optima were determined, the strains were retested using two degree temperature intervals near the optima. The NaCl requirement for each organism was determined by varying the NaCl content of the succinate supplemented basal medium recipes. The unmodified media both contained 2% NaCl (w/v). We inoculated from these 2% NaCl media into media containing different NaCl levels from 0 to 6%.

Determination of fermentation products. Fermentation products were determined using a Hewlett Packard 1100 series high performance liquid chromatography system equipped with a 25 cm Microsorb-MV C18 reversed-phase column (Rainin/Varian) and using a 0.01 N H_2SO_4 mobile phase at a flow rate of 1 ml · min^{-1}. Detection was by absorbance at 210 nm. Retention times of products were compared to those of known standard compounds, including acetate, propionate, and butyrate. Compound quantification was based on absorbances of known quantities of authentic compounds. Fermentation products were determined during early and late exponential phase, again during early stationary phase, and finally late in stationary phase.

Dehalogenation assays. Dehalogenation was determined at timed intervals throughout growth by measuring dehalogenation products by HPLC. Samples (1 ml) were taken and mixed with an equal volume of 100% acetonitrile. After centrifugation to remove precipitated proteins and polysaccharides, the samples were assayed for bromophenols using the Hewlett Packard 1100 series HPLC system with a 15 cm HP C18 reversed-phase column and using a methanol:H_2O:acetic acid (50:49:1) mobile phase at a flow rate of 1.5 ml · min^{-1}. Detection was measured by absorbance at 280 nm. Retention times of dehalogenation products were compared to those of authentic standard compounds, including 2-bromophenol, 4-bromophenol, 2,4-dibromophenol, 2,6-dibromophenol, and 2,4,6-tribromophenol (TBP). Compound quantification was based on absorbances of known quantities of authentic compounds.

Determination of mol% G + C content. DNA was isolated using a modification of the Marmur (1961) procedure, adding a cetyltrimethylammmonium bromide extraction step for removal of

contaminating polysaccharides and proteins (Ausubel *et al.*, 1987). The mol% G + C contents of each strain were determined after P1 nuclease digestion and HPLC separation of nucleosides (Mesbah *et al.*, 1989; Whitman *et al.*, 1986).

16S rDNA sequence determination and analysis. Genomic DNA was extracted and the gene coding for 16S rRNA (16S rDNA) was amplified as described previously (Rainey *et al.*, 1996). Purified PCR products were directly sequenced using the Taq DyeDeoxy Terminator Cycle Sequencing Kit (Applied Biosystems). Sequence reactions were electrophoresed using Applied Biosystems models 373A and 310 DNA sequencers. BLAST analysis was preformed on the sequence data to determine the phylogenetic grouping to which the strains were most closely related (Altschul *et al.*, 1990). The 16S rDNA sequences of strains DSL-1 and ML-1 were manually aligned with sequences of representatives of the low G+C Gram positive subphylum using the ae2 editor and sequence similarity values calculated by pairwise sequence comparison (Maidak *et al.*, 1994). The 16S rDNA sequences determined in this study are available from EMBL under the accession numbers Y16799 (strain DSL-1) and Y16800 (strain ML-1).

RESULTS AND DISCUSSION

Phylogenetic analyses. 16S rDNA sequences comprising 1441 nucleotides between positions 31 and 1493 (*Escherichia coli* numbering) were determined for strains DSL-1 and ML-1. Comparative analysis of the 16S rDNA sequences with those sequences available for representatives of the major bacterial groups using BLAST analyses indicated that both strains

were members of the low G+C Gram type positive subphylum. Alignment of the two sequences with those available for the members of the low G+C Gram type positive subphylum and analysis of all nucleotide positions showed them to be most closely related to members of the genus *Propionigenium*. The 16S rDNA sequence of strain DSL-1 was found to have 99.7% similarity to that of strain ML-1. The 16S rDNA sequence similarity between strain DSL-1 and *P. maris* was 99.6% while that to *P. modestum* was 96.0%. The 16S rDNA sequence of strain ML-1 had 99.9% similarity to *P. maris* and 95.7% to *P. modestum*.

Characterization of strains DSL-1 and ML-1.

Cell morphology. Cells of strain DSL-1 in exponential growth phase were short rods averaging 1 μm in length and 0.5 μm in diameter (Table 1). Stationary phase cells were shorter, some almost spherical (Figure 1). This strain displayed asymmetric cell division, with one daughter cell noticeably larger than the other during stationary phase (Figure 1). Strain ML-1 was also rod shaped and 0.5 μm in diameter, but cell length during exponential growth was variable, ranging from 2 to 10 μm. Both strains became shorter and more uniform during stationary phase, with ML-1 length averaging 2 μm in length. ML-1 did not display asymmetric cell division. Sporulation was not observed in either strain and is not a property of the genus *Propionigenium* (Schink & Pfennig, 1982). Strain ML-1 contained dense inclusions that were most numerous in stationary phase cells (Figure 2). No such inclusions were found in DSL-1 in any growth phase.

Gram stain reaction. The Gram stain reaction was negative but electron microscopy of osmium tetraoxide stained thin sections revealed a single dark-staining cell envelope layer (data not

shown), consistent with a Gram type positive cell wall structure. No lipopolysaccharide (LPS), the characteristic compound of Gram type negative cell walls, was detected using the LPS-polymyxin B assay of Wiegel & Quandt (1982). Other *Propionigenium* strains also stain Gram negative (Schink & Pfennig, 1982).

Growth properties. Both strains were obligately anaerobic. The pH range for growth of strain DSL-1 was 6.5 to 8.5, with optimal growth at pH 7.5-7.8. The pH range supporting growth of strain ML-1 was 5.5 to 7.5, and the optimum pH was 7.0. The lower pH optimum for strain ML-1 may reflect the stagnant conditions in *N. lobatus* burrows (Steward *et al.*, 1996). Burrow stagnation permits accumulation of volatile fatty acids (chiefly propionate, lactate, and acetate) produced by the worm under conditions of anaerobiosis (Schöttler *et al.*, 1983; Surholt, 1977) and consequently, substantial decreases in burrow water pH (Scott 1976). The temperature range for growth of strain DSL-1 was 10 to 35° C, and the optimum temperature was 30° C. The optimum temperature for growth of strain ML-1 was similar, 32° C. The shortest doubling times observed for strains DSL-1 and ML-1 at optimum pH and growth temperature were 0.30 - 0.32 h. Strain DSL-1 grew well within a NaCl concentration range of 1-5% with optimal growth at 2-3% NaCl and no growth at 0 or 6%. Strain ML-1 grew well from 1-4% NaCl with optimal growth at 3% and no growth at 0 or 5%. These results are consistent with the salinities observed in the euhaline saltmarsh environment from which these strains were isolated. The only defined carbon sources that were utilized in the presence of 0.05% yeast extract were pyruvate and succinate for strain DSL-1 and glucose and succinate for strain ML-1. The growth rate of strain DSL-1 was increased over that in the basal medium by addition of succinate or pyruvate at

concentrations up to 20 mM, but not above, while the growth rate of strain ML-1 was increased by succinate at concentrations up to 40 mM. Substrates that did not measurably increase the growth rate of either strain in the presence of 0.05% yeast extract included acetate, benzoate, citrate, crotonate, ethanol, fumarate, lactate, malate, oxalate, and propionate. In addition, strain DSL-1 did not utilize glucose and ML-1 did not utilize pyruvate. Strain DSL-1 growing on either pyruvate or succinate showed exponential decline in cell numbers in stationary phase. In the absence of these supplemental carbon sources the decline in stationary phase cell numbers was less marked. A similar effect was observed for glucose-grown strain ML-1, which goes into exponential decline after stationary phase. These stationary phase cultures could not always be successfully subcultured. Strain ML-1 cultures grown with succinate could be successfully subcultured after as long as 4 months if they were kept at room temperature. No appreciable change in growth rate or yield of either strain resulted from addition of nitrate, fumarate, or thiosulfate as potential terminal electron acceptors. The fermentation product of strain DSL-1 at all growth stages was butyrate. Strain ML-1 consistently produced propionate. Similar to strain ML-1, the *P. maris* type strain (DSM 9537) utilizes succinate and glucose (as well as several other substrates), requires yeast extract, and consistently produces propionate as its fermentation product (Janssen & Liesack, 1995).

Debromination. Tribromophenol was rapidly debrominated by both strains (Steward *et al.*, 1995 and Figure 3). DSL-1 produced primarily 2-bromophenol as the terminal debromination product; ML-1 produced a mixture of 2-bromophenol and 4-bromophenol. The discrepancy between the previous report of 4-bromophenol production by strain DSL-1 (Steward *et al.*, 1995)

and the current observation of 2-bromophenol is difficult to explain since in both cases the product identities were confirmed by mass spectroscopy. This change may be due to a change in the culture between the initial determinations and the present work. Neither strain could utilize 2- or 4-bromophenol as carbon substrates. 3-bromophenol was not tested. Neither strain dechlorinated chlorophenols. Similar substrate spectra, i.e. the capacity to debrominate but not to dechlorinate the corresponding chlorinated compounds, has been observed with 2,4,6-tribromobiphenyl dehalogenating enrichment cultures (Chuang, 1997). However, the corresponding 2,4,6-trichlorobiphenyl dehalogenating enrichment could dehalogenated both the chlorinated and structurally analogous brominated compounds (Chuang, 1997), indicating the presence of at least two different assemblages of dehalogenating bacteria, of which one could only debrominate.

Bromophenols supplied at millimolar concentrations did not affect yield or doubling time. The absence of growth stimulation or change in growth yields indicates that debromination by these strains does not lead to energy production. This is in contrast to the dehalogenation of chloro(bromo)phenols by the Gram type positive, sulfite reducing *Desulfitobacterium dehalogenans*, which was isolated from freshwater sediments, and in which dehalogenation leads to 1 ATP formed for each reductively removed halogen atom and thus to increased growth yields in comparison to the fermentation of pyruvate. The energy is presumably coupled to electron transport phosphorylation. This mechanism enables this dehalogenating bacterium to grow on hydrogen and formate while using the halogenated phenols as electron acceptors (Mackiewicz & Wiegel, 1998). The debromination of 2,4-dibromobiphenyl also supports enhanced growth of

reductively dehalogenating microorganisms in sediment samples (Wu *et al.*, 1999). *P. maris*, the closest related organism to the two novel isolates based on 16S rDNA sequence analysis, was also tested for dehalogenation activity. Growth of unadapted *P. maris* type strain DSM 9537 was strongly inhibited by 1 mM TBP. After adaptation through successive subculturing using media containing 100 μM through 500 μM TBP, type strain DSM 9537 could be grown in the presence of up to 500 μM TBP and trace amounts of the debromination terminal product, 2-bromophenol, were detected. No indication of growth stimulation or evidence that debromination is coupled to energy production were obtained for any *P. maris* strains. *Propionigenium* species are regarded as purely fermentative anaerobes (Schink & Pfennig, 1982; Janssen & Liesack, 1995). No increases in cell yields by *P. modestum* (Schink & Pfennig 1982) or any strain of *P. maris* in response to added nitrate, fumarate, or thiosulfate has been observed. This indicates that no energy yielding electron transport phosphorylation system is functioning in these species.

G+C content. The G+C content of genomic DNA from DSL-1 is 39 ± 0.3 mol% (SD, n = 6), 41 ± 0.1 mol% (SD, n = 4) for ML-1 DNA. These values are in good agreement with G+C contents of other *Propionigenium* strains (Table 1).

In conclusion, the high 16S rDNA sequence similarity found between strains DSL-1 and ML-1 and the two described species of the genus *Propionigenium* clearly indicate their membership in the genus *Propionigenium*. Based on similarities to the *P. maris* type strain and phylogenetic analysis we currently place the new isolates as novel strains in the species *Propionigenium maris*. The new strains have a high degree of 16S rDNA sequence similarity to that of the *P.*

maris type strain (99.6-99.9%), but differ from the latter organism in several physiological features including cell size, substrate preferences, temperature and pH optima and, most importantly, ability to rapidly debrominate TBP. The infaunal burrow, a dynamic microenvironment that supports high bacterial biomass and activities, may promote rapid evolution of these *Propionigenium* strains, resulting in substantial physiological variability without concurrent changes in 16S rDNA sequence. Our identification of these isolates as strains of *P. maris* is conservative and based in large measure on 16S rDNA sequence homology.

The new *P. maris* strains have been isolated from infaunal burrows with important differences in several microenvironmental features. The size, shape, and placement in the sediments of the burrows, the texture and organic matter content of sediment in the burrow linings, and the porosity of the surrounding sediments (which affects solute transport rates) all differ (see Steward *et al.*, 1996 for further discussion). The feeding modes of the host invertebrates, their irrigation behaviors, and, likely, the availability of organic substrates released by the hosts differ as well. Given the great variety of burrowing marine invertebrate taxa, the many types of burrow structures they build, and their range of microbiologically significant behaviors (burrow maintenance activities, irrigation regimes, feeding strategies, etc.) it is probable that many distinct strains of *P. maris*, and likely new *Propionigenium* species, occur in marine infaunal burrows. Burrows of bromometabolite producing infauna may also harbor additional dehalogenating strains and species. Further work is needed for evaluation of the importance of this group of organisms.

Emendation. The species description for *P. maris* (Janssen & Liesack, 1995) is emended for the property of reductive dehalogenation of bromophenols found in the linings of some marine infaunal burrows. In contrast to strains isolated from the burrows, which are regarded as a special habitat for some *P. maris* strains, the type strain DSM 9537 exhibits only minor debromination activity and only after prolonged adaptation. Furthermore, some strains may not utilize sugars and butyrate can be the major fermentation product from pyruvate and succinate, although the type strain forms propionate as the major product from glucose and succinate. Depending on the isolate, the cell size varies between 0.5 and 1 μm in diameter and 1 and 10 μm in length.

ACKNOWLEDGEMENTS

We are grateful to W.B. Whitman for help with determination of the mol% G + C contents of DSL-1 and ML-1. This research was supported by the Office of Naval Research, grant number N00014-96-0403 to C.R.L.

REFERENCES

Abrahamsson, K. & Klick, S. (1991). Degradation of halogenated phenols in anoxic natural marine sediments. *Mar Pollut Bull* **22**, 227-233.

Allard, A.-S., Hynning, P.-A., Lindgren, C., Remberger, M. & Neilson, A. H. (1991). Dechlorination of chlorocatechols by stable enrichment cultures of anaerobic bacteria. *Appl Environ Microbiol* **57**, 77-84.

Altschul, S. F., Gish, W., Miller, W., Myers, E. W. & Lipman, D. J. (1990). Basic local alignment search tool. *J Mol Biol* **215**, 403-410.

Ausubel, F.M., Brent, R., Kingston, R. E., Moore, D. D., Seidman, J. G., Smith, J. A. & Struhl, K. (1987). *Current protocols in molecular biology.* New York, NY: Wiley.

Boothe, D. D. H., Rogers, J. E. & Wiegel, J. (1997). Reductive dechlorination of chlorophenols in slurries of low-organic-carbon marine sediments and subsurface soils. *Appl Microbiol Biotechnol* **47**, 742-748.

Chen, Y. P., Lincoln, D. E., Woodin, S. A. & Lovell C. R. (1991). Purification and properties of a unique flavin-containing chloroperoxidase from the capitellid polychaete *Notomastus lobatus*. *J Biol Chem* **266**, 23909-23915.

Chuang, K.-S. (1997). Anaerobic transformation of polyhalogenated biphenyls in freshwater sediments from Woods Pond. MS thesis, University of Georgia, Athens GA (USA)

El Fantroussi, S., Naveau, H. & Agathos, S. N. (1998). Anaerobic dechlorinating bacteria. *Biotechnol Prog* **14**, 167-188.

Fetzner, S. & Lingens, F. (1994). Bacterial dehalogenases: biochemistry, genetics, and biotechnological applications. *Microbiol Rev* **58**, 641-685.

Fielman, K. T. & Targett, N. M. (1995). Variation of 2,3,4-tribromopyrrole and its sodium sulfamate salt in the hemichordate *Saccoglossus kowalevskii*. *Mar Ecol Prog Ser* **116**, 125-136.

Fielman, K. T., Woodin, S. A., Walla, M. D. & Lincoln, D. E. (1999). Widespread occurrence of natural halogenated organics among temperate marine infauna. *Mar Ecol Prog Ser*, In press.

Genthner, B. R. S., Price, W. A. II & Pritchard, P. H. (1989). Anaerobic degradation of chloroaromatic compounds in aquatic sediments under a variety of enrichment conditions. *Appl Environ Microbiol* **55**, 1466-1471.

Häggblom, M. (1992). Microbial breakdown of halogenated aromatic pesticides and related compounds. *FEMS Microbiol Rev* **103**, 29-72.

Häggblom, M. M. & Young, L. Y. (1990). Chlorophenol degradation coupled to sulfate reduction. *Appl Environ Microbiol* **56**, 3255-3260.

Häggblom, M. M. & Young, L. Y. (1995). Anaerobic degradation of halogenated phenols by sulfate-reducing consortia. *Appl Environ Microbiol* **61**, 1546-1550.

Hale, D. D., Reineke, W. & Wiegel, J. (1994). Chlorophenol degradation. In: *Biological degradation and bioremediation technologies of toxic chemicals,* pp. 74-91. Edited by G. R. Chaudry. Portland, OR: Timber Press.

Holliger, C., Wohlfarth, G. & Diekert, G. (1999). Reductive dechlorination in the energy metabolism of anaerobic bacteria. *FEMS Microbiol Rev* **22**, 383-398.

Janssen, P. H. & Liesack, W. (1995). Succinate decarboxylation by *Propionigenium maris* sp. nov., a new anaerobic bacterium from an estuarine sediment. *Arch Microbiol* **164**, 29-35.

Janssen, D. B., Pries, F. & van der Ploeg, J. R. (1994). Genetics and biochemistry of dehalogenating enzymes. *Annu Rev Microbiol* **48**, 163-191.

King, G. M. (1986). Inhibition of microbial activity in marine sediments by a bromophenol from a hemichordate. *Nature* **323**, 257-259.

King, G. M. (1988). Dehalogenation in marine sediments containing natural sources of halophenols. *Appl Environ Microbiol* **54**, 3079-3085.

Löffler, F. E., Sanford, R. A. & Tiedje, J. M. (1996). Initial characterization of a reductive dehalogenase from *Desulfitobacterium chlororespirans* Co23. *Appl Environ Microbiol* **62**, 3809-3813.

Lovell, C. R., Steward, C. C. & Phillips, T. (1999). Activity of marine sediment bacterial communities exposed to 4-bromophenol, a polychaete secondary metabolite. *Mar Ecol Prog Ser*, In press.

Mackiewicz, M. & Wiegel, J. (1998). Comparison of energy and growth yields for *Desulfitobacterium dehalogenans* when utilizing chlorophenol and various traditional electron acceptors. *Appl Environ Microbiol* **64**, 352-355.

Maidak, B. L., Larsen, N., McCaughey, M. J., Overbeek, R., Olsen, G. J., Fogel, K., Blandy, J. & Woese, C. R. (1994). The Ribosomal Database Project. *Nucleic Acids Res* **22**, 3485-3487.

Marmur, J. (1961). A procedure for the isolation of deoxyribonucleic acid from micro-organisms. *J Mol Biol* **3**, 208-218.

Mesbah, M., Premachandran, U. & Whitman, W.B. (1989). Precise measurement of the G + C content of deoxyribonucleic acid by high-performance liquid chromatography. *Int J Syst Bacteriol* **39**, 159-167.

Mohn, W. W. & Tiedje, J. M. (1992). Microbial reductive dehalogenation. *Microbiol Rev* **56**, 482-507.

Monserrate, E. & Häggblom, M. M. (1997). Dehalogenation and biodegradation of brominated phenols and benzoic acids under iron-reducing, sulfidogenic, and methanogenic conditions. *Appl Environ. Microbiol* **63**, 3911-3915.

Neilson, A. H. (1990). The biodegradation of halogenated organic compounds. *J Appl Bacteriol* **69**, 445-470.

Ni, S., Fredrickson, J. K. & Xun, L. (1995). Purification and characterization of a novel 3-chlorobenzoate-reductive dehalogenase from the cytoplasmic membrane of *Desulfomonile tiedjei* DCB-1. *J Bacteriol* **177**, 5135-5139.

Phillips, T. M. & Lovell, C. R. (1999). Distributions of total and active bacteria in biofilms lining tubes of the onuphid polychaete *Diopatra cuprea*. *Mar Ecol Prog Ser*, In press.

Rainey, F. A., Ward-Rainey, N., Kroppenstedt, R. M. & Stackebrandt, E. (1996). The genus

Nocardiopsis represents a phylogenetically coherent taxon and a distinct actinomycete lineage: proposal of *Nocardiopsaceae* fam. nov. *Int J Syst Bacteriol* **46**, 1088-1092.

Remberger, M., Allard, A.-S. & Neilson, A. H. (1986). Biotransformations of chloroguaiacols, chlorocatechols, and chloroveratroles in sediments. *Appl Environ Microbiol* **51**, 552-558.

Schink, B. & Pfennig, N. (1982). *Propionigenium modestum* gen. nov., sp. nov., a new strictly anaerobic, nonsporing bacterium growing on succinate. *Arch Microbiol* **133**, 209-216.

Schöttler, U., Wienhausen, G. & Zebe, E. (1983). The mode of energy production in the lugworm *Arenicola marina* at different oxygen concentrations. *J Comp Physiol* **149**, 547-555.

Scott, D. M. (1976). Circadian rhythm of anaerobiosis in a polychaete annelid. *Nature* **262**, 811-813.

Steward, C. C. & Lovell, C. R. (1997). Respiration and assimilation of 4-bromophenol by estuarine sediment bacteria. *Microb Ecol* **33**, 198-205.

Steward, C. C., Pinckney, J., Piceno, Y. & Lovell, C. R. (1992). Bacterial numbers and activity, microalgal biomass and productivity, and meiofaunal distribution in sediments naturally contaminated with biogenic bromophenols. *Mar Ecol Prog Ser* **90**, 61-71.

Steward, C. C., Dixon, T. C., Chen, Y. P. & Lovell, C. R. (1995). Enrichment and isolation of a reductively debrominating bacterium from the burrow of a bromometabolite-producing marine hemichordate. *Can J Microbiol* **41**, 637-642.

Steward, C. C., Nold, S. C., Ringelberg, D. B., White, D. C. & Lovell, C. R. (1996). Microbial biomass and community structures in the burrows of bromophenol producing and non-producing marine worms and surrounding sediments. *Mar Ecol Prog Ser* **133**, 149-165.

Surholt, B. (1977). Production of volatile fatty acids in the anaerobic carbohydrate metabolism in the lugworm *Arenicola marina* L. *Comp Biochem Physiol* **58B**: 147-150.

Tschech, A. & Pfennig, N. (1984). Growth yield and increase linked to caffeate reduction in *Acetobacterium woodii*. *Arch Microbiol* **137**, 163-167.

Utkin, I.., Dalton, D. D. & Wiegel, J. (1995). Specificity of reductive dechlorination of substituted ortho-chlorophenols by *Desulfitobacterium dehalogenans* JW/IU-DC1. *Appl Environ Microbiol* **61**, 346-351.

Whitman, W. B., Sohn, S., Caras, D. S. & Premachandran, U. (1986). Isolation and characterization of 22 mesophilic methanococci. *Syst Appl Microbiol* **7**, 235-240.

Wiegel, J. & Quandt, L. (1982). Determination of the Gram type using the reaction between

polymyxin B and lipopolysaccharides of the outer cell wall of whole bacteria. *J Gen Microbiol* **128**, 2261-2270.

Woodin, S. A., Walla, M. D. & Lincoln, D. E. (1987). Occurrence of brominated compounds in soft-bottom benthic organisms. *J Exp Mar Biol Ecol* **107**, 209-217.

Wu, Q., Bedard, D. & Wiegel, J. (1999). 2,6-dibromobiphenyl primes extensive dechlorination of Aroclor 1260 in contaminated sediment at 8 to 30°C by stimulating growth of PCB dehalogenating microorganisms. *Environ Sci Technol*, In press.

Yoon, K. S., Chen, Y. P., Lovell, C. R., Lincoln, D. E., Knapp, L. W. & Woodin, S. A. (1994). Localization of the chloroperoxidase of the capitellid polychaete *Notomastus lobatus*. *Biol Bull* **187**, 215-222.

Table 1. Selected properties of *Propionigenium maris* strains. *P. modestum* is included for comparison.

Property	*P. maris* DSL-1	*P. maris* ML-1	*P. maris*[*] DSM 9537	*P. modestum*[†]
Cell size (μm)[‡]	1 x 0.5	2 x 0.5	2.5 x 1	2 x 0.5
Inclusions	none	present	none	none
Carbon substrates	succinate pyruvate	succinate glucose	succinate pyruvate fumarate citrate 3-hydroxy-butyrate glucose fructose maltose	succinate pyruvate fumarate malate oxaloacetate L-aspartate
Fermentation Products[§]	butyrate	propionate	propionate (butyrate) (acetate) (lactate) (formate) (ethanol)	propionate (acetate)
Optimum pH	7.5-7.8	7.0	6.9-7.7	7.1-7.7
Optimtum temperature (°C)	28	32	34-37	33
Mol% G+C	39	41	40	33.9

[*] Data from reference Janssen & Liesack (1995).
[†] Data from reference Schink & Pfennig (1982).
[‡] Cell dimensions (length x width) for exponentially growing cells. All *Propionigenium* cells are rods
[§] Production of butyrate, acetate, lactate, formate, and ethanol by *P. maris* and acetate by *P. modestum* is dependent on the carbon source.

FIGURE LEGENDS

Figure 1. Phase contrast photomicrograph of *Propionigenium maris* strain DSL-1 during stationary phase. Note asymmetric cell division (arrows).

Figure 2. Phase contrast photomicrograph of *Propionigenium maris* strain ML-1 during stationary phase. Note inclusions (arrows).

Figure 3. Growth (A) and debromination of 2,4,6-tribromophenol (B) by *Propionigenium maris* strain ML-1. (Open circles) 2,4,6-tribromophenol, (closed squares) 2,4-dibromophenol, (open triangles) 4-bromophenol, (closed triangles) 2-bromophenol. Values are means of three cultures incubated in parallel. Error bars represent one standard deviation. For symbols with no error bars, error bars are smaller than the symbols.

Watson et al. Fig. 1

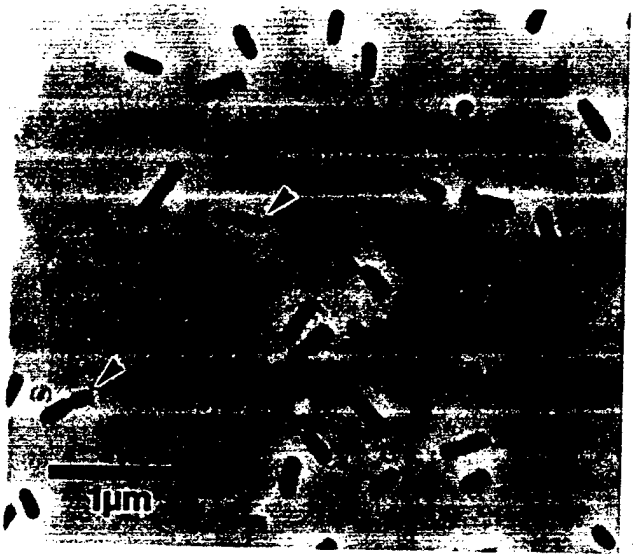

Watson
et al.
Fig. 2

Watson et al. Fig. 3

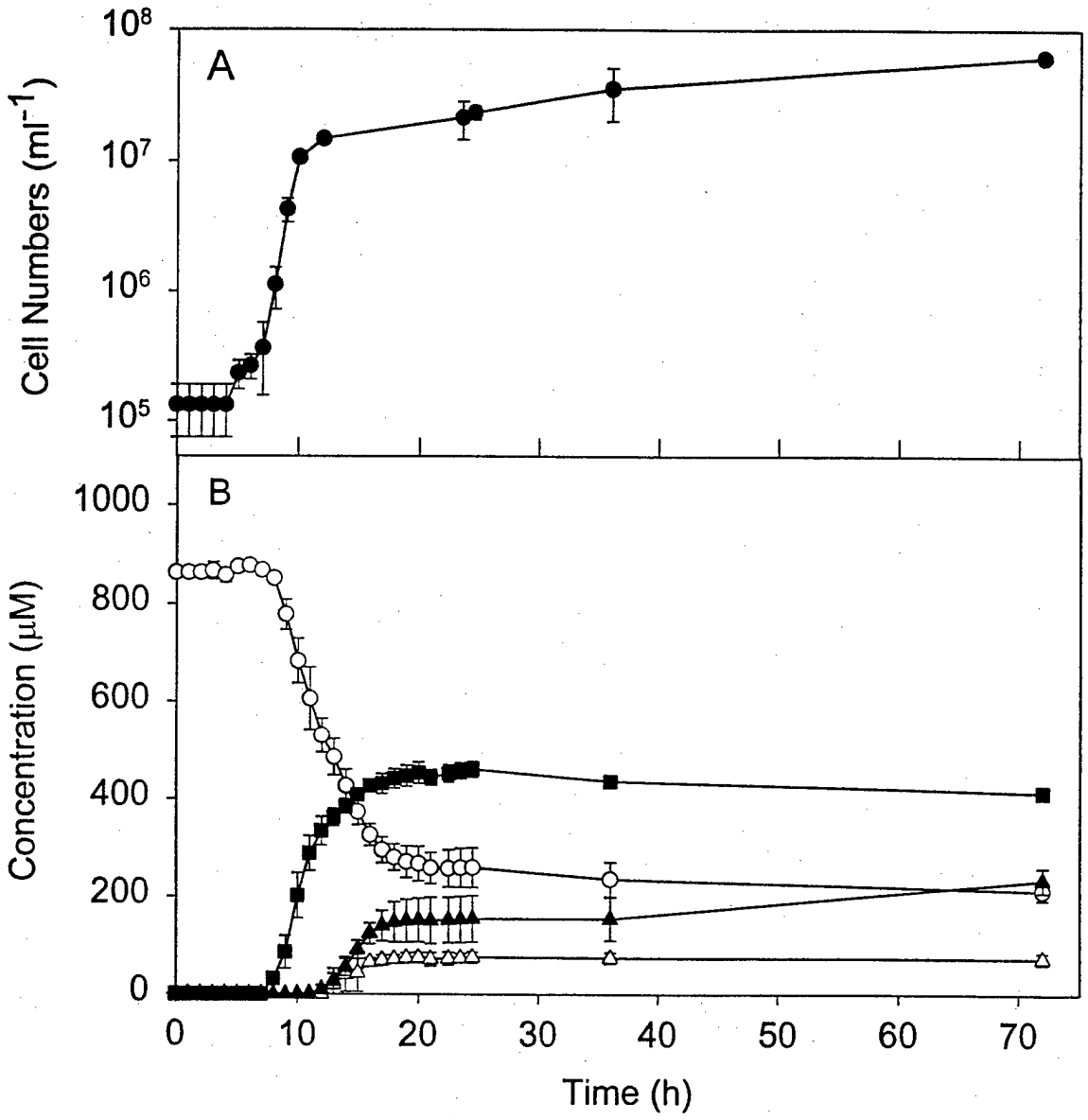

OFFICIAL ABSTRACT FORM

98TH ASM GENERAL MEETING ◆ ATLANTA, GEORGIA ◆ MAY 17–21, 1998

Instructions: Complete this form and submit it for receipt by 5:00 p.m. (EST), December 19, 1997. Any poorly prepared abstract unsuitable for direct reproduction will not be reviewed by the GMPC.

Type the category in here (see pp. 12-14) ☞ N4

A FONT NO SMALLER THAN 10 POINT IS REQUIRED.

Type here: ☞
the title (initial capitals only)
all authors (in all capital letters)
affiliations (short addresses only)
abstract text (Do not place tables, figures, grant acknowledgments, or references in text.)

Effects of host activities on the composition of microbial communities in biofilms lining burrows of marine infauna.

C. R. LOVELL*[1], R. L. MARINELLI[2], S. G. WAKEHAM[2], D. G. RINGELBERG[3], AND D. C. WHITE[4]. [1]Univ. South Carolina, Columbia, SC, [2]Skidaway Inst. Oceanography, Savannah, GA, [3]Waterway Experiment Station, Vicksburg, MS, and [4]Univ. Tennessee, Knoxville, TN.

Marine infaunal burrows provide conditions highly conducive to microbial activity and are sites of high biogeochemical reaction rates. These unique microenvironments facilitate development of biofilm microbial communities quite different from those in the surrounding sediments. Differences among biofilm communities growing in burrows with differing structures have also been observed. We have conducted a series of manipulative experiments and used phospholipid fatty acid (PLFA) analysis to examine the impact of host activities on the composition of burrow lining biofilm microbial communities. We found that the compositions of these communities were strongly affected by the irrigation activities of the infaunal host organism and the residence time of the burrows in sediments. PLFA profiles showed that immature biofilms were dominated by aerobic bacteria while mature biofilms contained both aerobes and anaerobes. Among numerous anaerobe PLFAs, the signature compound for *Desulfobacter*, 10me16:0, was particularly responsive to irrigation regime and to age of the burrow. Our results show that two aspects of infaunal host behavior, irrigation frequency and mobility, may have major impacts on the biogeochemistry of nearshore sediments.

Check here if you are a predoctoral student and are interested in being considered for an ASM Sustaining Member Student Travel Grant (must meet eligibility criteria).

Complete checklist and sign the back of this form before submitting abstract.

Abstracts submitted via facsimile will not be accepted by the Program Committee.

Keyword 1: Community_structure
Keyword 2: marine_infauna
Keyword 3: biofilms

Presenting Author Information:

1461771
(pending, if membership application is enclosed)

First name: Charles
MI: R.
Last name: Lovell
Institution: University of South Carolina
Department: Department of Biological Sciences
Mailing Address, line 1: Coker Life Sciences
Mailing Address, line 2:
City: Columbia
State/Prov.: SC
ZIP Postal Code: 29208
Country: USA
Phone: (803)777-7036
E-mail address: lovell@biol.sc.edu
Fax: (803)777-4002

Mail abstract to:

General Meeting Abstracts
American Soc. for Microbiology
1325 Massachusetts Ave, NW
Washington, DC 20005-4171

OFFICIAL ABSTRACT FORM

98TH ASM GENERAL MEETING ◆ ATLANTA, GEORGIA ◆ MAY 17–21, 1998

Instructions: Complete this form and submit it for receipt by 5:00 p.m. (EST), December 19, 1997. Any poorly prepared abstract unsuitable for direct reproduction will not be reviewed by the GMPC.

Type the category in here (see pp. 12-14) ☞ N4

A FONT NO SMALLER THAN 10 POINT IS REQUIRED.

Type here:
the title (initial capitals only)
all authors (in all capital letters)
affiliations (short addresses only)
abstract text (Do not place tables, figures, grant acknowledgments, or references in text.)

Distribution of Bacterial Cells and Biomass in *Diopatra cuprea* Burrow Lining Biofilms

T. M. PHILLIPS* AND C. R. LOVELL. Univ. of South Carolina, Columbia, SC

Macrofaunal burrows contain high levels of microbial biomass and support rapid rates of significant geochemical processes. These burrows are dug into anoxic subsurface sediments, irrigated with oxic seawater, and provide a large surface for diffusive exchange. As a consequence, they are ideal sites for development of microbial biofilms. Using scanning confocal laser microscopy we examined the distribution of bacterial cell numbers and biomass, estimated average cell sizes, and determined the potentially active fraction of bacteria in biofilms lining the tubes of the onuphid polychaete *Diopatra cuprea*. The thickness of the biofilm for 49 vertical profiles within 5 burrows ranged from 30 μm to 110 μm (average: 60 μm). The average number of bacterial within a burrow ranged from 2.4 – 6.8 x 10^8 cells/cm^3. Twenty-five of the profiles had highest cell numbers within the first 10 μm from the surface of the biofilm. Twenty-three had additional subsurface peaks in cell numbers. In 32 of the 49 profiles, the largest average cell size was within the first 10 μm from the surface. Nineteen profiles showed subsurface peaks in average cell size. Twenty-four profiles had highest biomass within the first 10 μm from the surface. Twelve profiles had subsurface peaks in biomass. Potentially active cells were present at all depths within the biofilm with no characteristic depth having a high proportion of inactive cells. Surface layers had a higher proportion of dead cells in many but not all cases. Multicellular aggregates and small colonies also were found at all depths within the biofilm. Bacterial cells and biomass within burrow lining biofilms are not distributed homogenously or concentrated primarily at specific depths.

Check here if you are a predoctoral student and are interested in being considered for an ASM Sustaining Member Student Travel Grant (must meet eligibility criteria).

Complete checklist and sign the back of this form before submitting abstract.

Abstracts submitted via facsimile will not be accepted by the Program Committee.

Biofilms | Marine Infauna | Bacterial Distribution

Presenting Author Information:

55188171
(pending, if membership application is enclosed)

Tina | M | Phillips
University of South Carolina
Biological Sciences
Coker Life Sciences 408
Columbia | SC | 29208
USA | 803-777-5153
tcoleman@biol.sc.edu | 803-777-4002

Mail abstract to:

General Meeting Abstracts
American Soc. for Microbiology
1325 Massachusetts Ave, NW
Washington, DC 20005-4171